Bridging experimental and observational realms in gravitational-wave searches

Francesco Di Renzo - IP2I, Lyon   f.di-renzo@ip2i.in2p3.fr

Outlook of the presentation

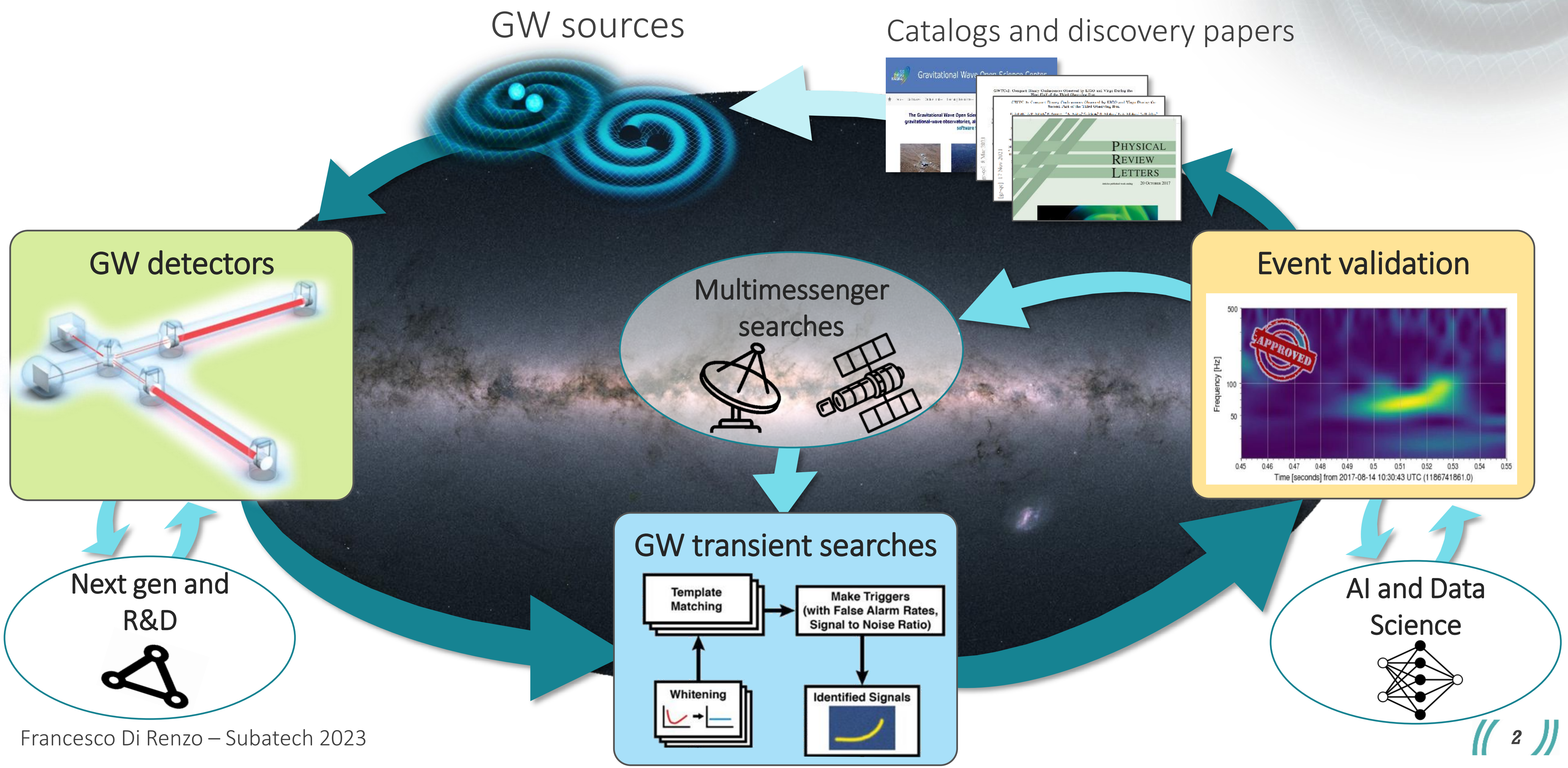

Prelude: compact binary observations by LIGO and Virgo

Masses in the stellar graveyard

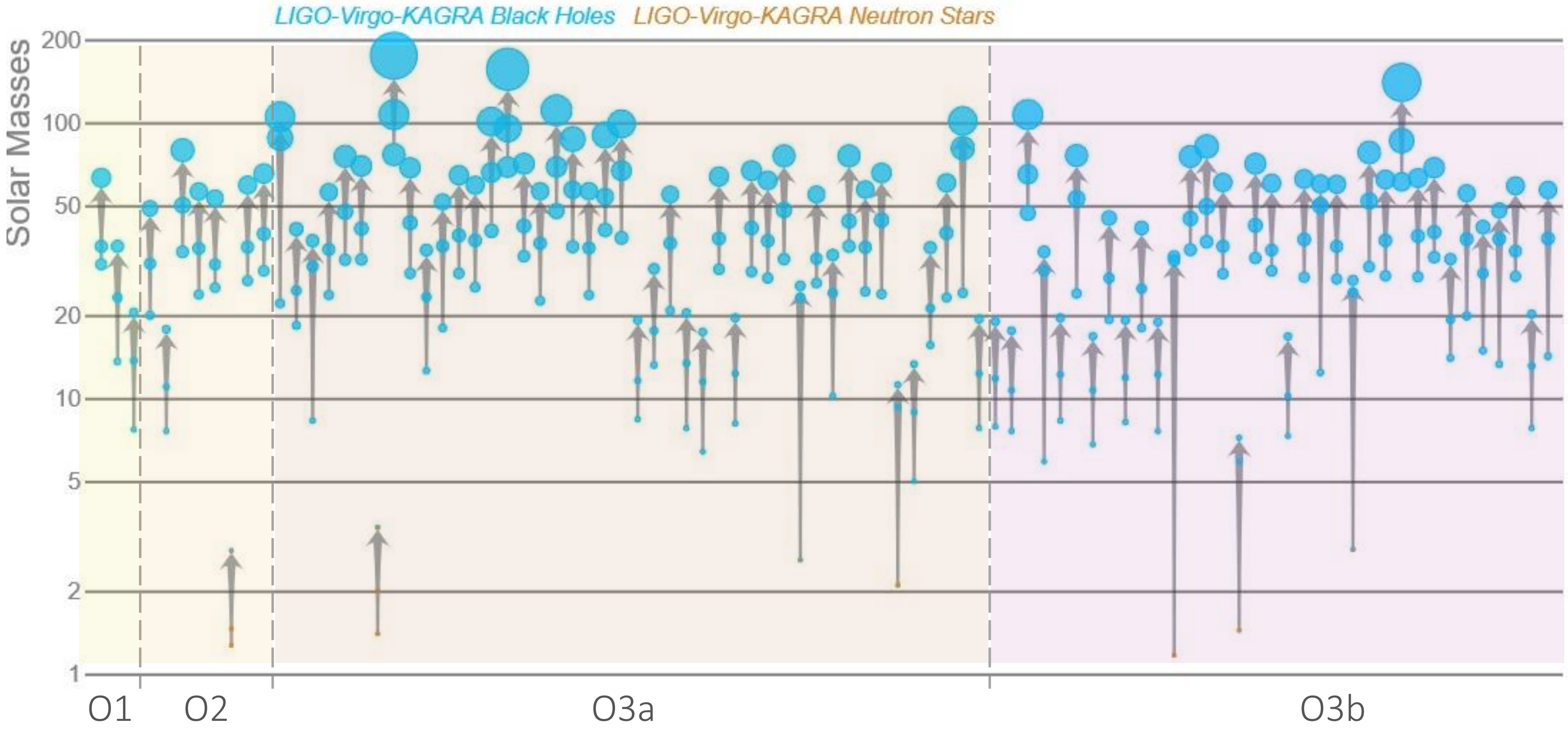

Credit: Visualization: LIGO-Virgo-KAGRA / Aaron Geller / Northwestern

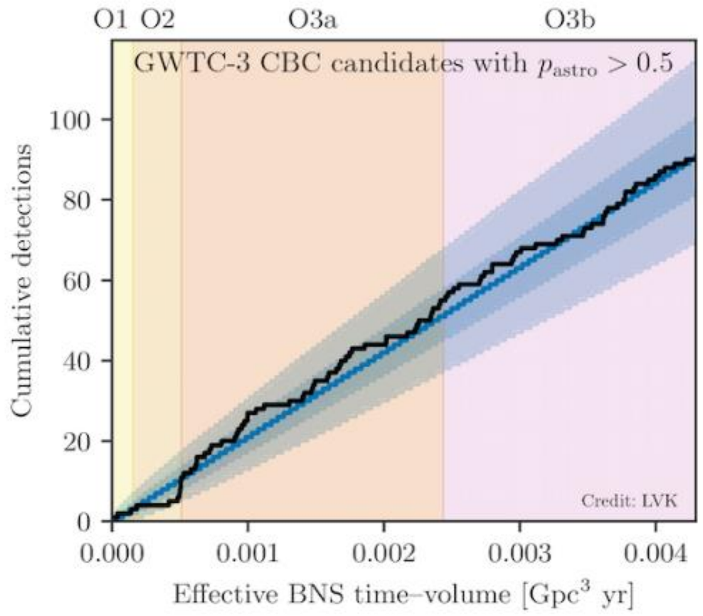

arXiv:2111.03606

Interferometric Gravitational-Wave Detectors

- The Advanced detectors LIGO, Virgo and KAGRA
- Basics of interferometric GW detectors
- Noise sources vs. sensitivity

The global network of gravitational-wave detectors

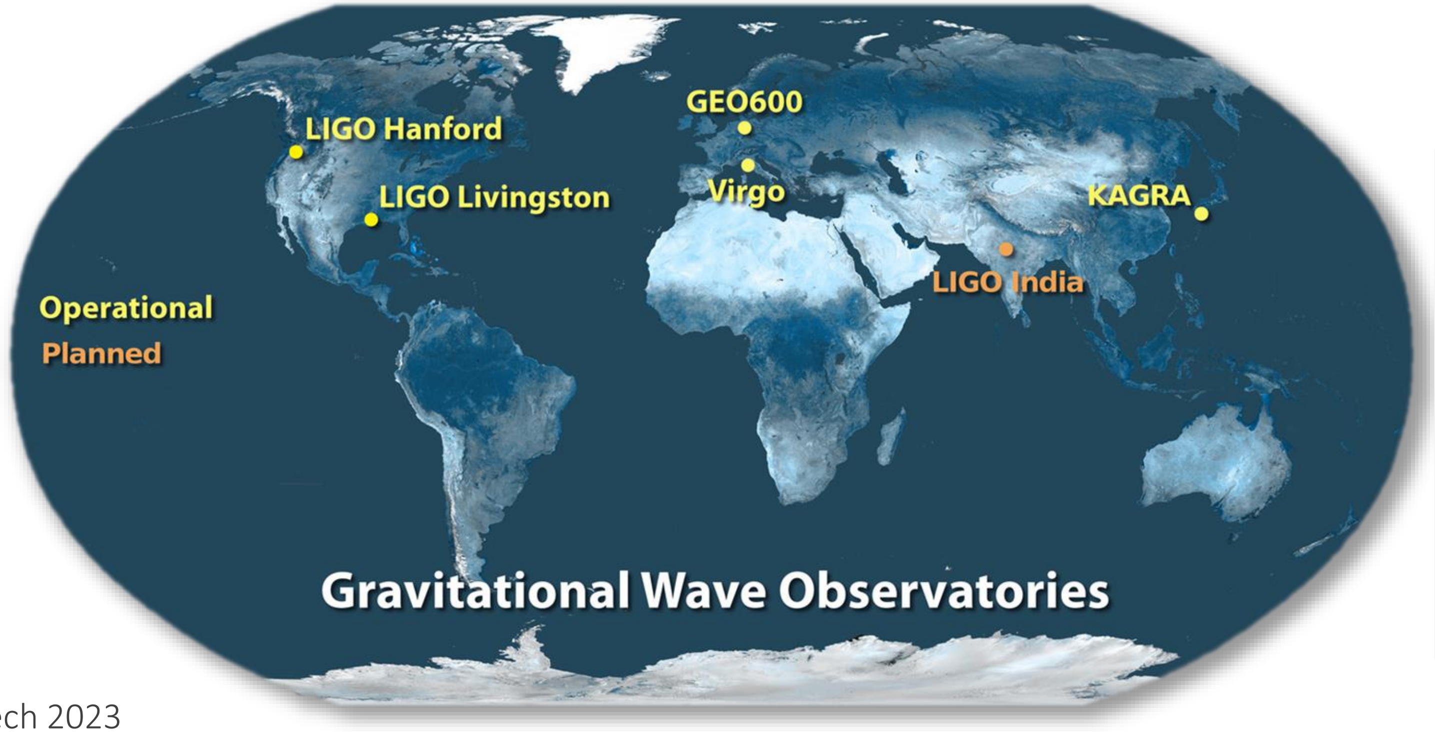

The LVK in numbers

LIGO Scientific Collaboration

- Founded in 1997
- 127 institutions
- 1600 individuals
- 19 countries

Virgo Collaboration

- Founded in 1994
- 140 institutions
- 800 individuals
- 16 countries

KAGRA Collaboration

- Founded in 2010
- 110 institutions
- 400 individuals
- 15 countries

Interferometric gravitational-wave detectors (I)

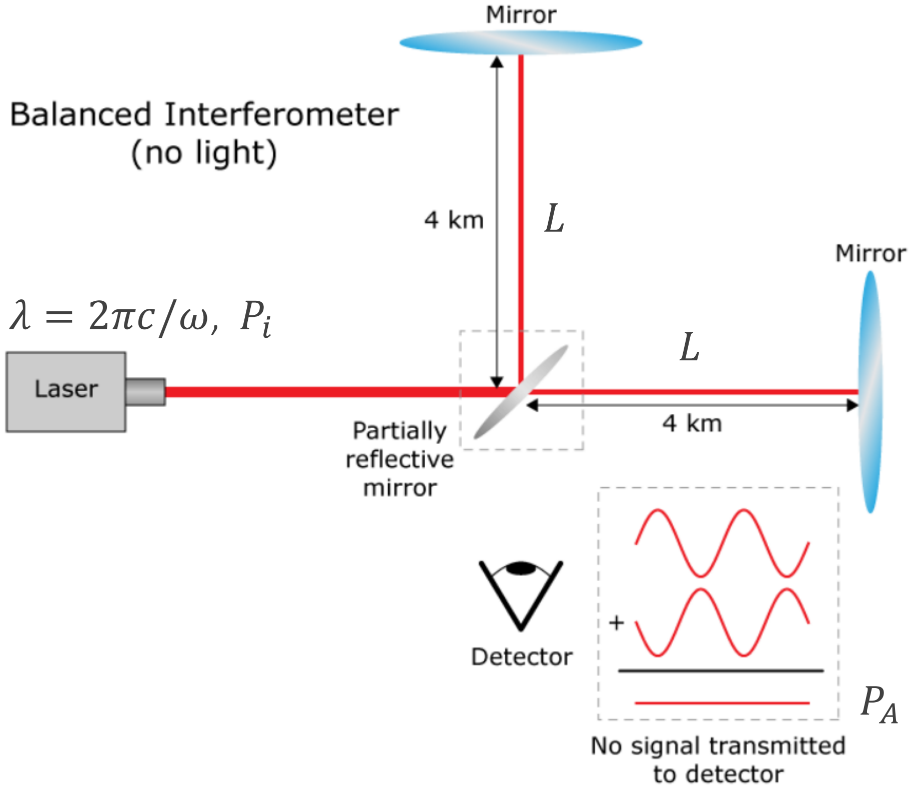

Image credit: *Michael Gerhardt*

- Effect of a GW signal on the detector arms:

$$\delta L_{GW} \approx h\, L$$

with h the **GW strain amplitude** and L the size of the detector.

Interferometric gravitational-wave detectors (I)

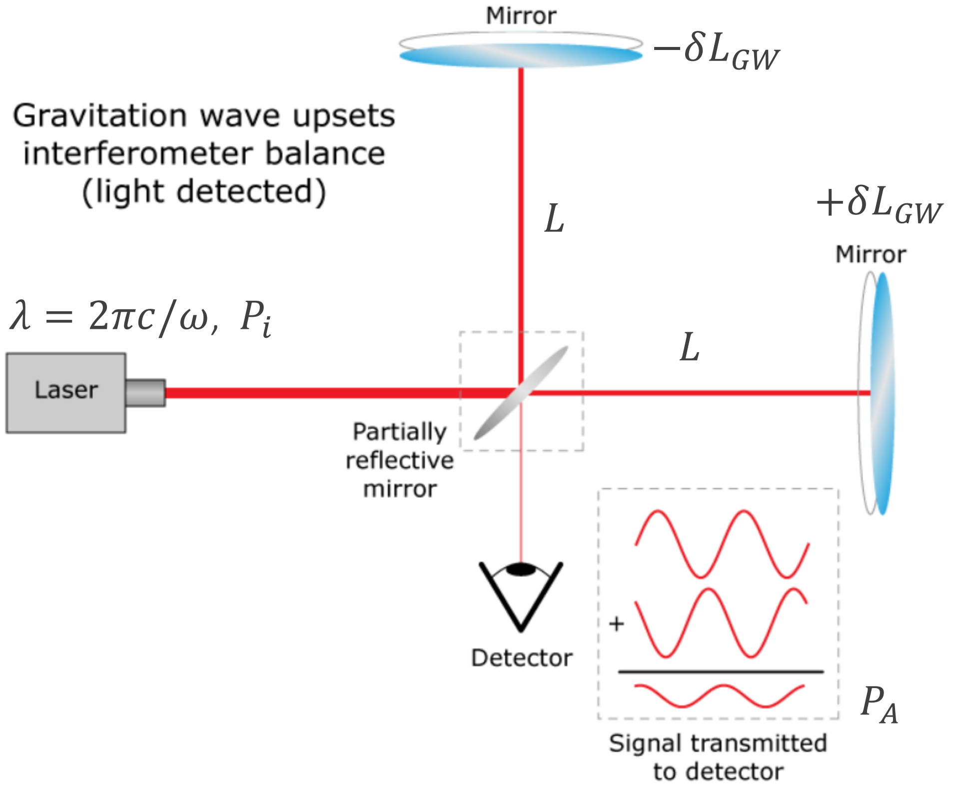

Image credit: *Michael Gerhardt*

- Effect of a GW signal on the detector arms:

$$\boldsymbol{\delta L_{GW} \approx h\, L}$$

  with h the **GW strain amplitude** and L the size of the detector.

- The power at the detector antisymmetric port is:

$$P_A \propto \frac{L}{\lambda} P_i\, h$$

  with λ the laser wavelength (e.g. 1 µm) and P_i the input power.

- We can characterize the detector sensitivity by mans of its **strain Amplitude Spectral Density ($\boldsymbol{S_h^{1/2}}$)**: $S_A^{1/2} \propto \frac{L}{\lambda} P_i\, S_h^{1/2}$.

- A "shot-noise limited" ($S_N^{1/2} = \sqrt{2\hbar\omega\, P_A}$) interferometric detector:

$$S_h^{1/2} \gtrsim \sqrt{\frac{\hbar c^2}{\omega}} \frac{1}{L\sqrt{P_i}}$$

  where ω is the laser angular frequency.

- The RHS gives the shot-noise limited **detector sensitivity**.

Interferometric gravitational-wave detectors (II)

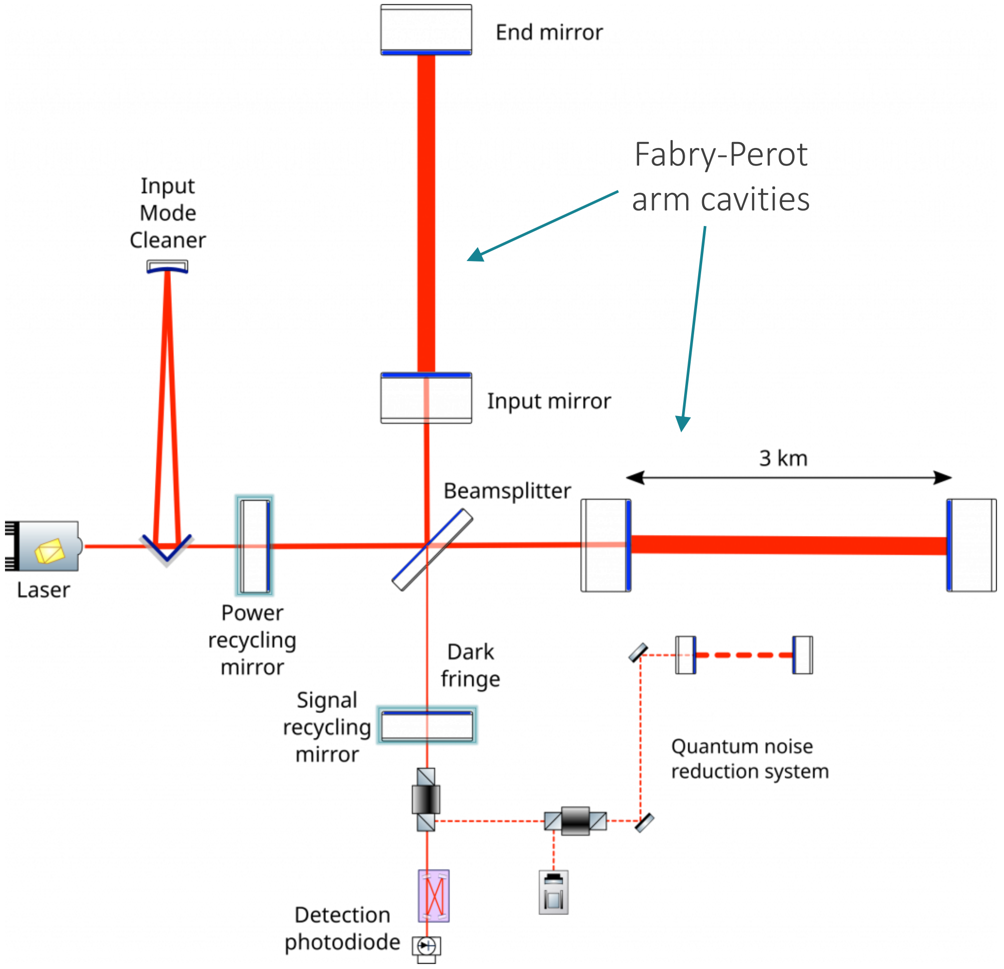

- Fabry-Perot arm cavities: increase the effective arm length by a factor $2\mathcal{F}/\pi$, with $\mathcal{F}$ the arm cavity *finesse* (~450)
- Power recycling: increase the circulating power by a factor G_{pr} (~35)
- Signal recycling cavity: move up the *cavity pole* ($f_p = c/4\mathcal{F}L$), increasing the detector bandwidth (Resonant signal extraction, RSE)

$$S_{SN}(f) = \frac{1}{(4\mathcal{F}L)^2}\frac{\hbar c^2}{\omega}\frac{1}{P_i\, G_{pr}}\frac{1}{g(f)}$$

with $g(f) = \left[1 + (f/f_p)^2\right]^{-1}$ the F-P arm cavity frequency response.

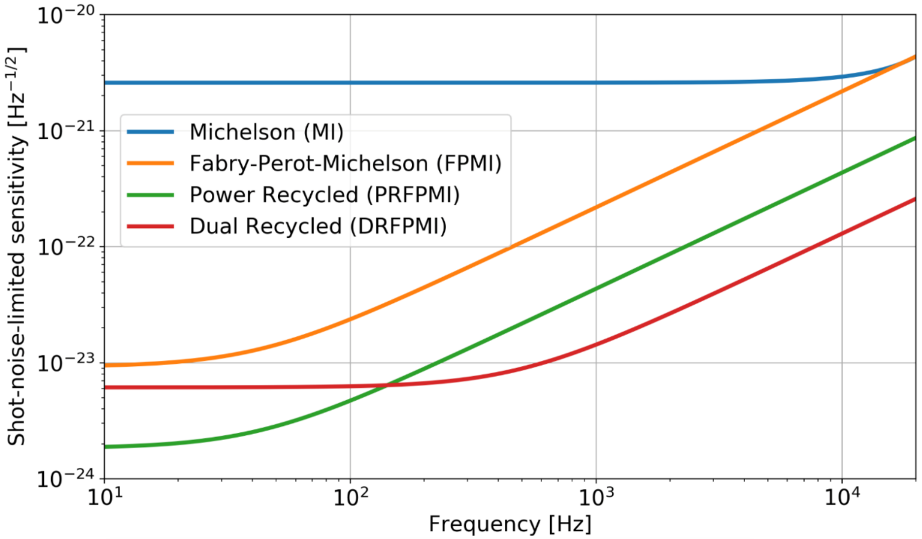

Image credit: *Gabriele Vajente*

Radiation pressure noise

- Photons carry a momentum: $p = E/c = \hbar\omega/c$
- A laser beam exerts a force on a mirror: $F_{RP} = P/c$
- This force fluctuates as the power ($S_P^{1/2} = \sqrt{2\hbar\omega\, P}$)
- Displacement ASD:

$$S_{RPN}^{1/2}(f) = \frac{\sqrt{\hbar\omega\, P/2}}{mc\,\pi^2 f^2}$$

with m the mirror mass (42 kg)

- GW detection as a quantum measurement problem
- Quantum Backaction on kg-scale Mirrors: Phys. Rev. Lett. 125 131101, Nature 583, 43–47 (2020)

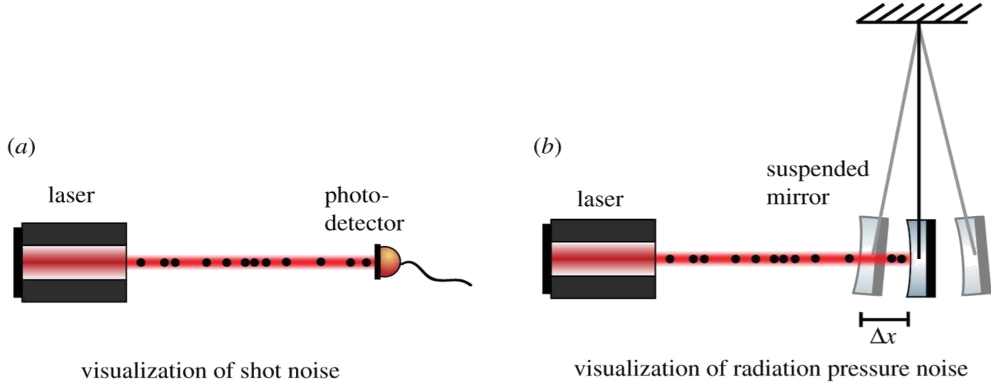

Sum of shot noise and radiation pressure for a simple Michelson interferometer

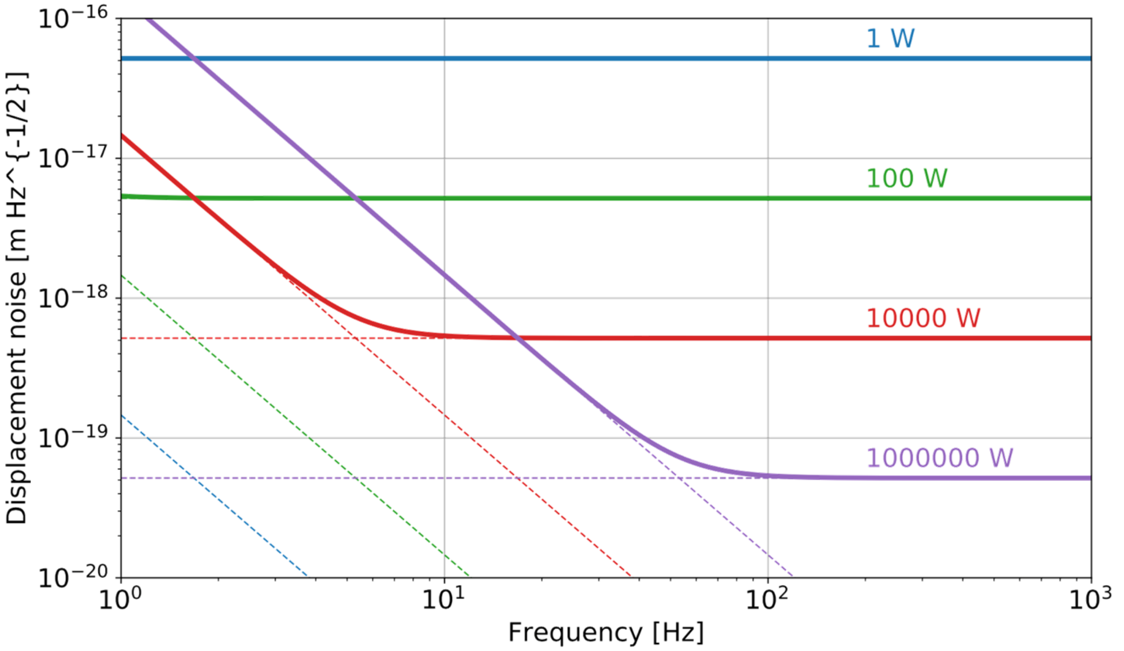

Image credit: *Gabriele Vajente*

Quantum-noise limited GW detector

$$S_{QN}(f) = S_{SN}(f) + S_{RPN}(f) = \frac{1}{(4\mathcal{F}L)^2}\frac{\hbar c^2}{\omega}\frac{1}{P_i\,G_{pr}}\frac{1}{g(f)} + \left(\frac{4\mathcal{F}}{M\pi^2}\right)^2\frac{2\hbar\omega}{f^4}\cdot P_i\,G_{pr}\cdot g(f)$$

While the shot-noise limited sensitivity improves with P, the radiation-pressure limited sensitivity gets worse with P.

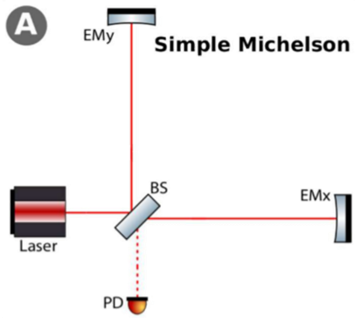

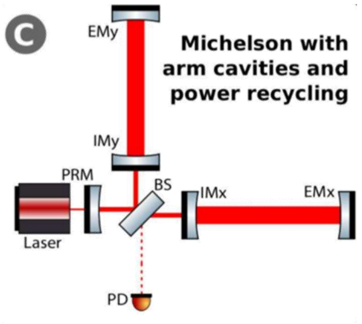

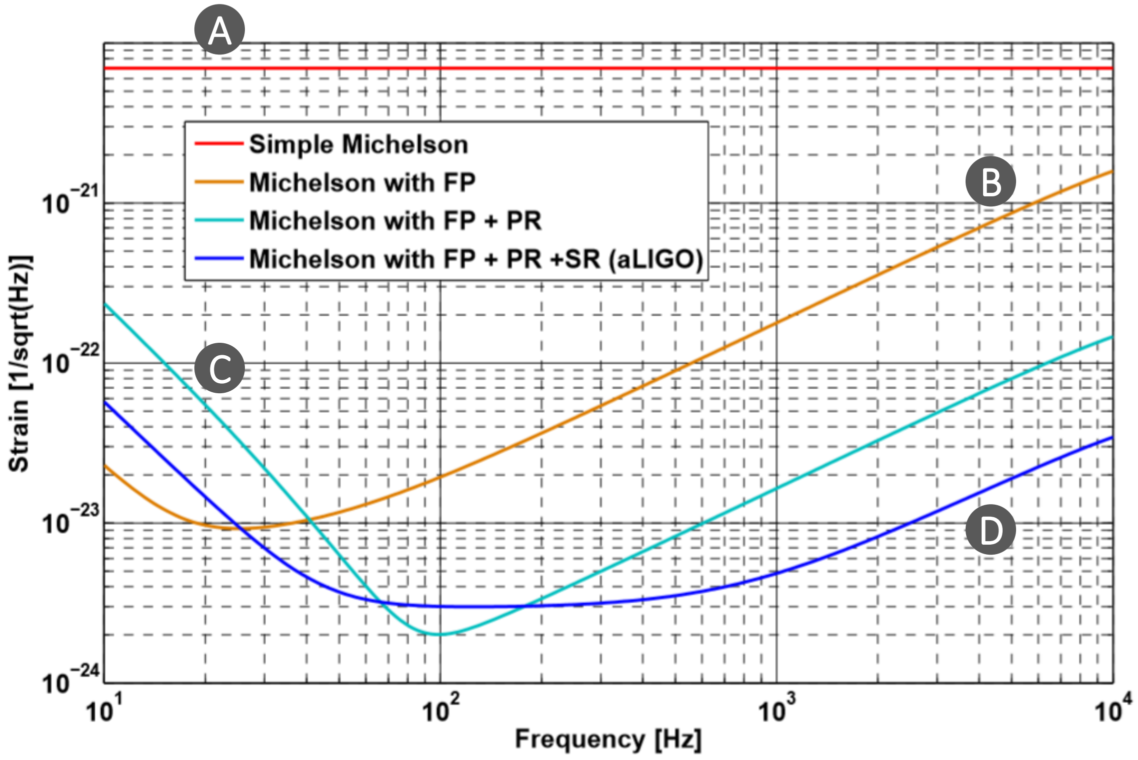

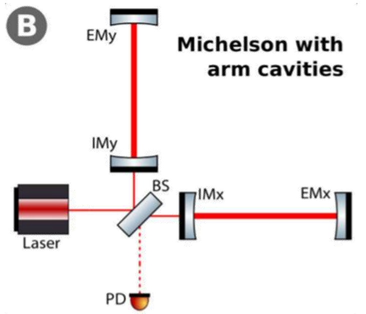

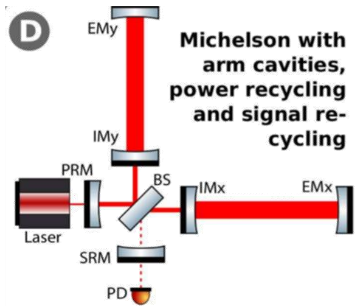

Beating the Standard Quantum Limit: Frequency-dependent Quantum Squeezing

$$S_{SQZ}(f) = S_{QN}(f)\,[e^{-2r}\cos^2(\phi - \theta(f)) + e^{2r}\sin^2(\phi - \theta(f))]$$

with r the squeeze factor and

$$\theta(f) = \tan^{-1}\left[\frac{4\mathcal{F}}{M\pi^2}\frac{\hbar\omega}{f^2}\cdot P_i\, G_{pr}\cdot g(f)\right].$$

For frequency-independent squeezing (for $\phi = 0$):

$$S_{SQZ}(f) = S_{SN}(f)\ e^{-2r} + S_{RPN}(f)\ e^{2r}$$

equivalent of increasing the power by a factor e^{2r}.

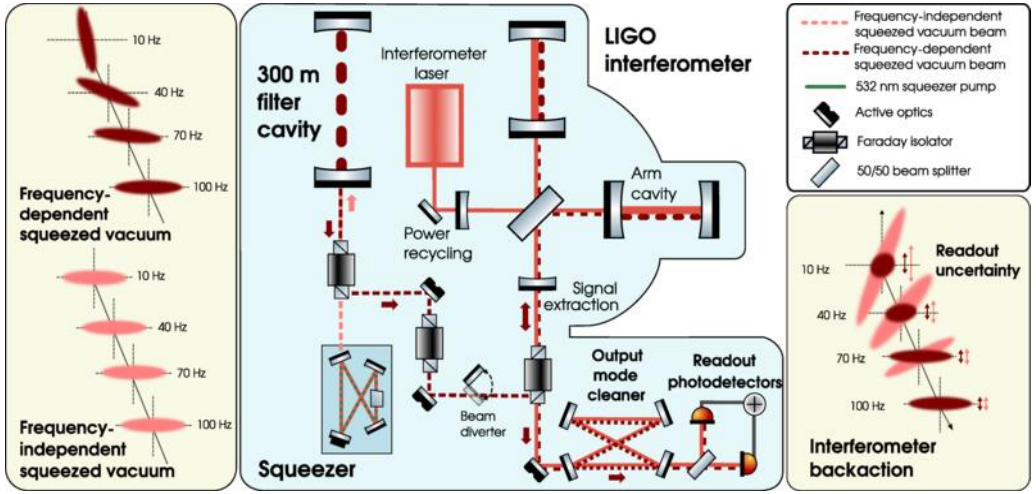

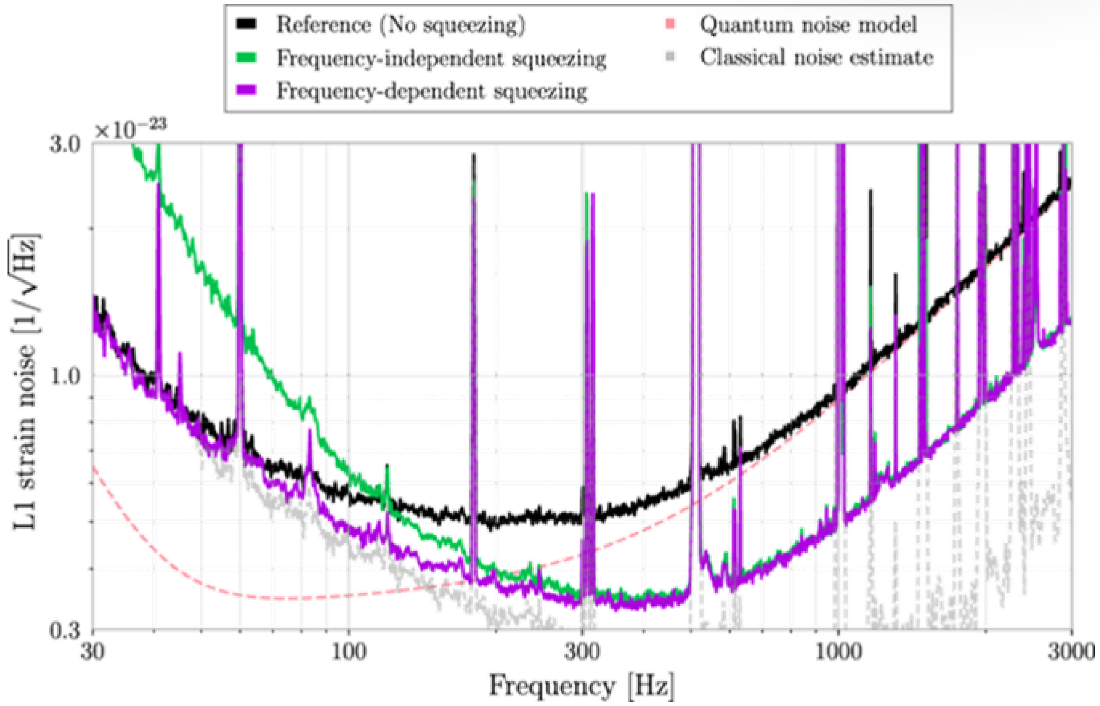

Phys. Rev. X 13, 041021

Real gravitational wave detectors

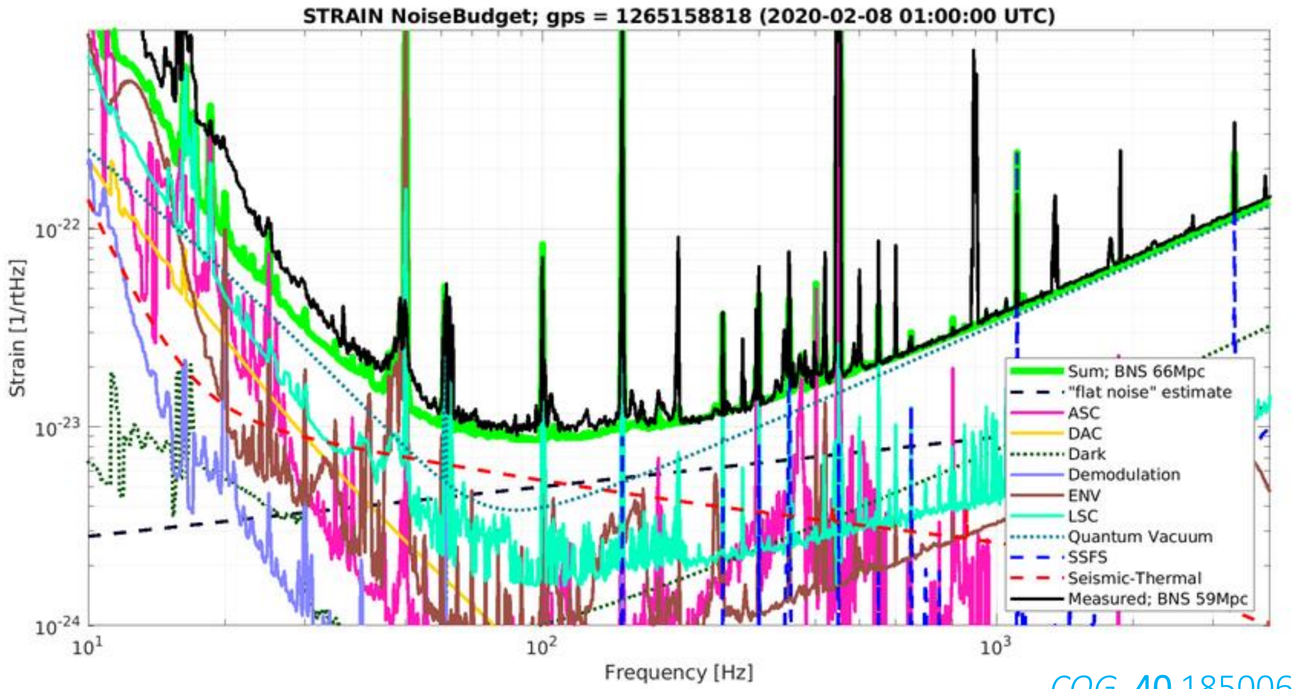

[CQG. 40 185006]

Snapshot of May 31, 2023

Five GW detectors simultaneously observing for the first time

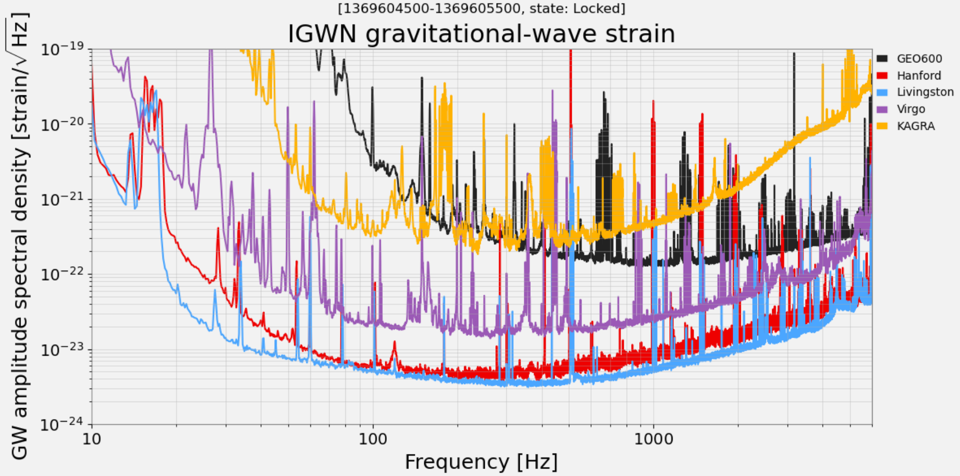

Many *non-astrophysical* sources can produce an effect similar to a strain at the detector output: **noise**

- **Fundamental noise:** intrinsic in the detection principle and its practical implementation
- **Technical noise:** from components and controls that are not optimal
- **Environmental noise:** from the detector physical environment

Detector noise and sensitivity to various sources

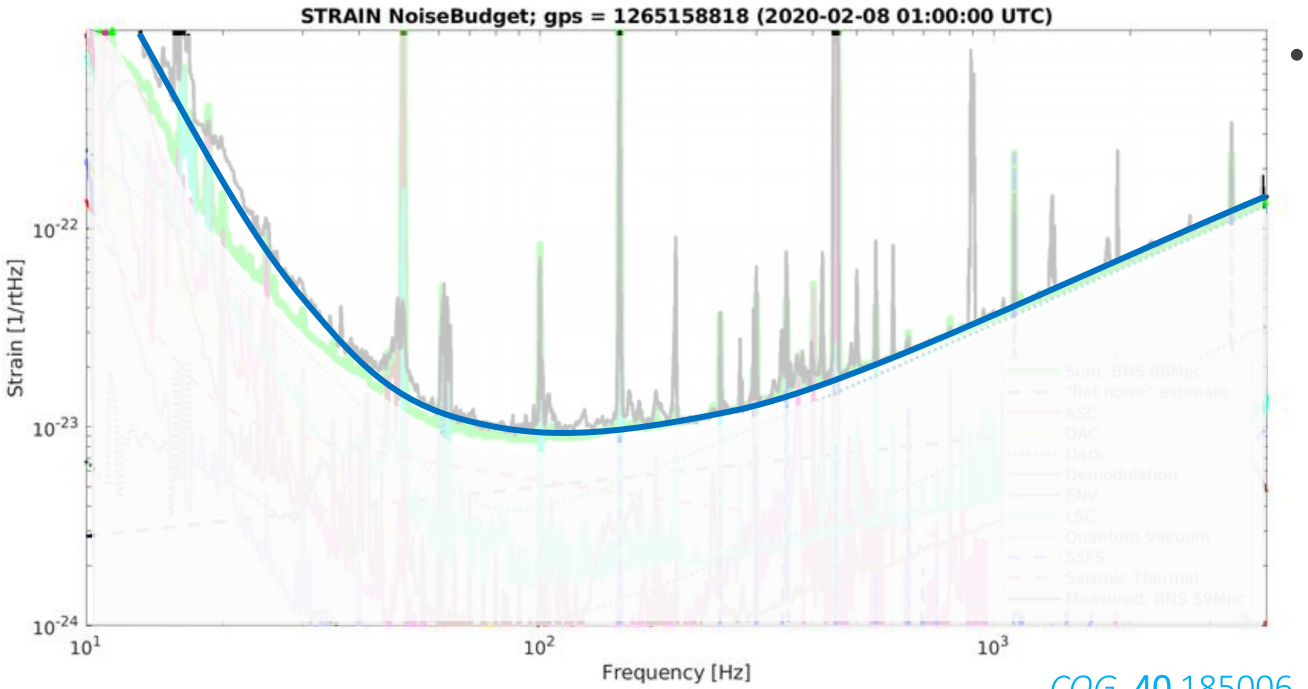

[*CQG.* **40** 185006]

- Strain sensitivity shape determines the detector range, namely how far a specific kind of source can be detected. E.g. BNS range

Many *non-astrophysical* sources can produce an effect similar to a strain at the detector output: **noise**

- **Fundamental noise:** intrinsic in the detection principle and its practical implementation
- **Technical noise:** from components and controls that are not optimal
- **Environmental noise:** from the detector physical environment

Detector noise and sensitivity to various sources

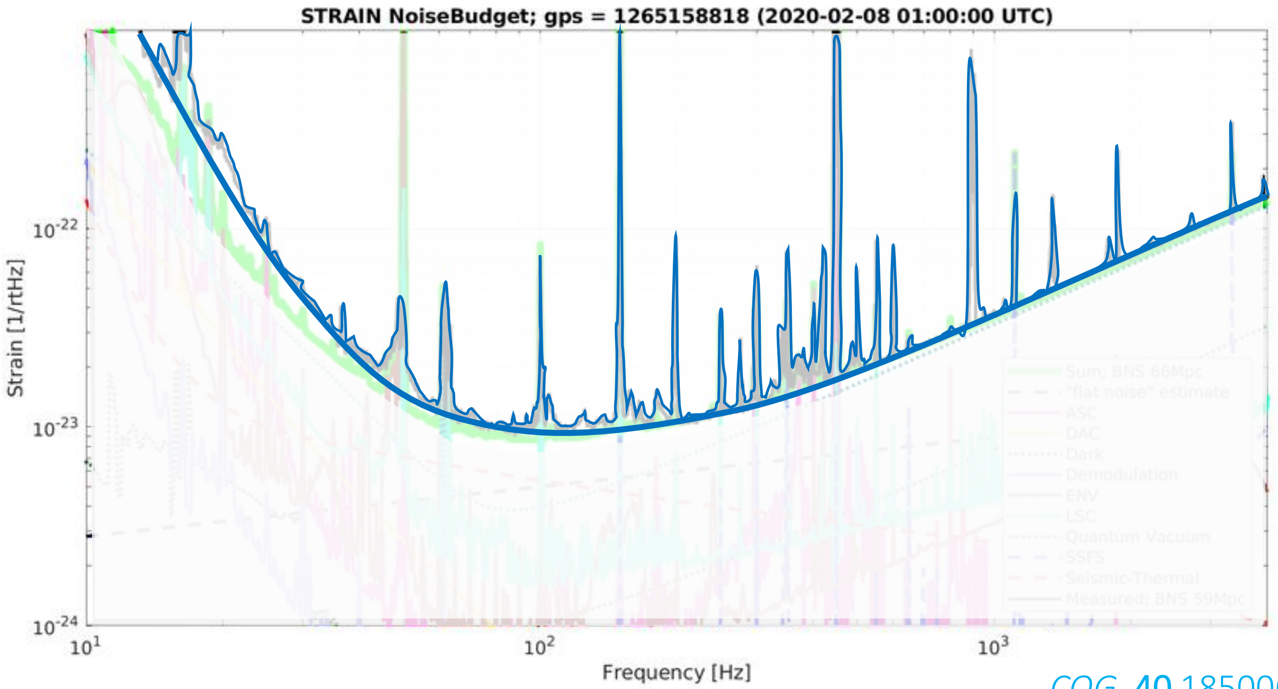

CQG. **40** 185006

- Strain sensitivity shape determines the detector range, namely how far a specific kind of source can be detected. E.g. BNS range
- Spectral lines reduce the sensitivity, in particular for narrow-band signals, e.g. continuous waves

Many *non-astrophysical* sources can produce an effect similar to a strain at the detector output: noise

- **Fundamental noise:** intrinsic in the detection principle and its practical implementation
- **Technical noise:** from components and controls that are not optimal
- **Environmental noise:** from the detector physical environment

Detector noise and sensitivity to various sources

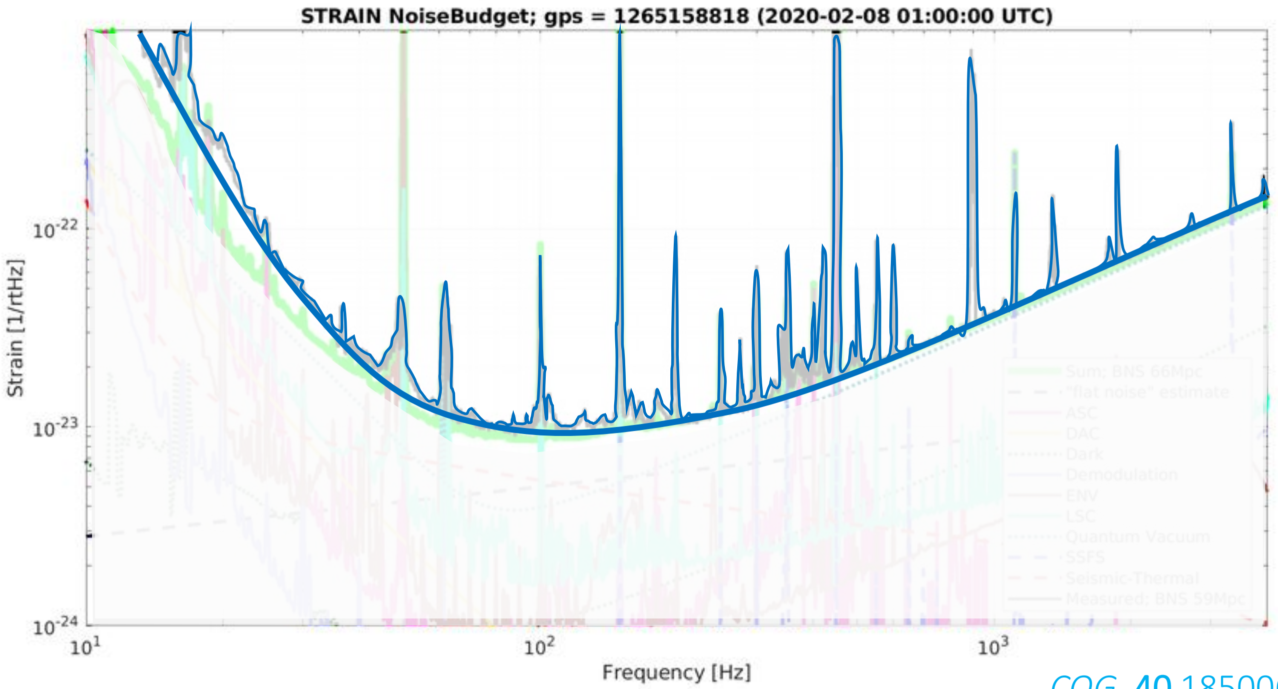

CQG. 40 185006

- Strain sensitivity shape determines the detector range, namely how far a specific kind of source can be detected. E.g. BNS range
- Spectral lines reduce the sensitivity, in particular for narrow-band signals, e.g. continuous waves
- Transient noise, colloquially called "glitches," can mimic transient GW signal or hinder their presence

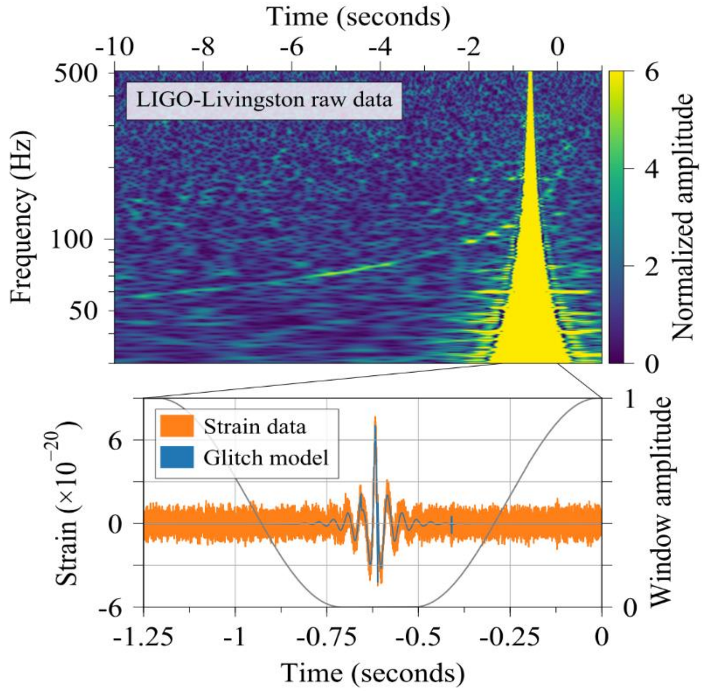

PRD 98 084016

Detector noise and sensitivity to various sources

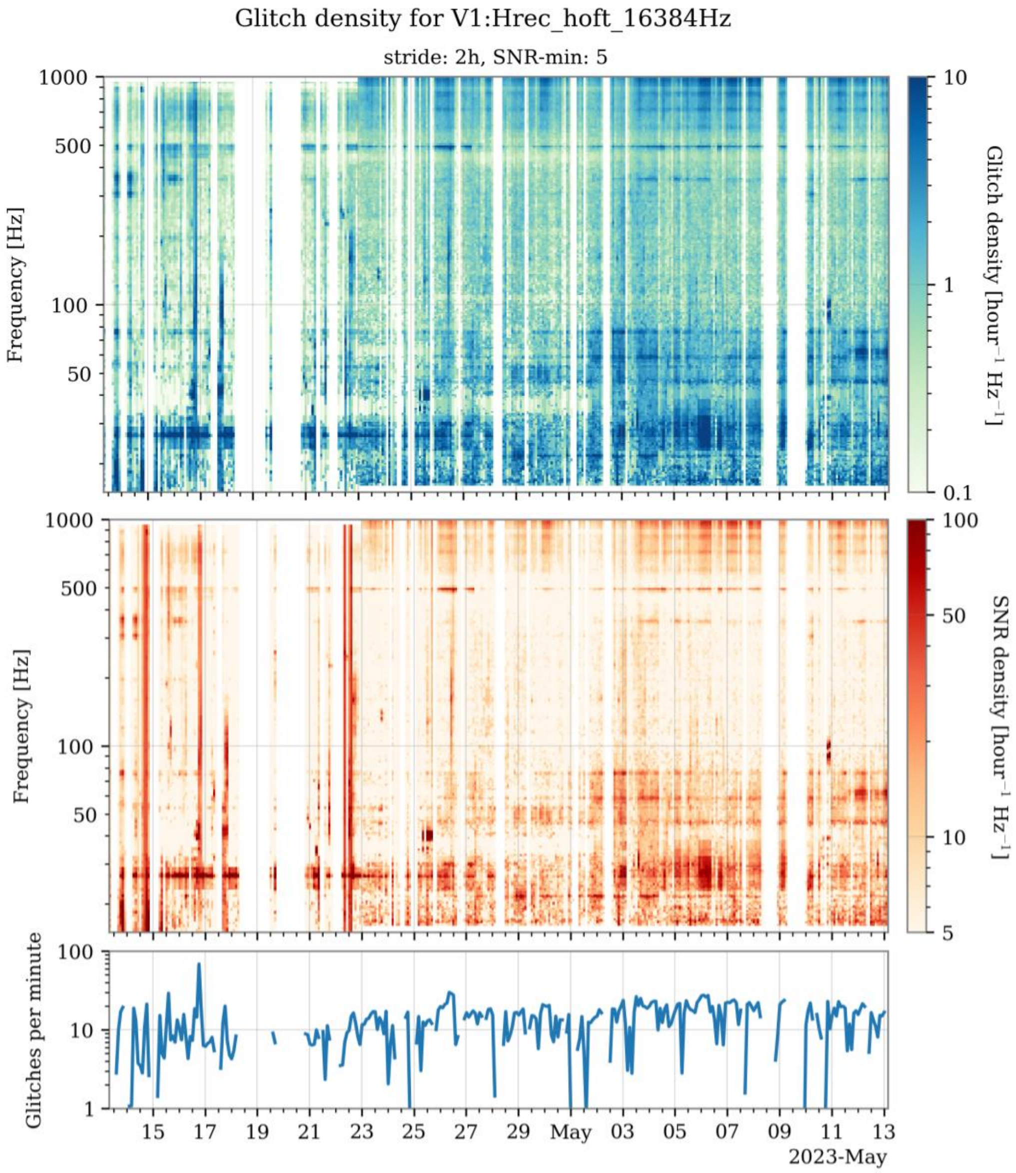

- Strain sensitivity shape determines the detector range, namely how far a specific kind of source can be detected. E.g. BNS range
- Spectral lines reduce the sensitivity, in particular for narrow-band signals, e.g. continuous waves
- Transient noise, colloquially called "glitches," can mimic transient GW signal or hinder their presence

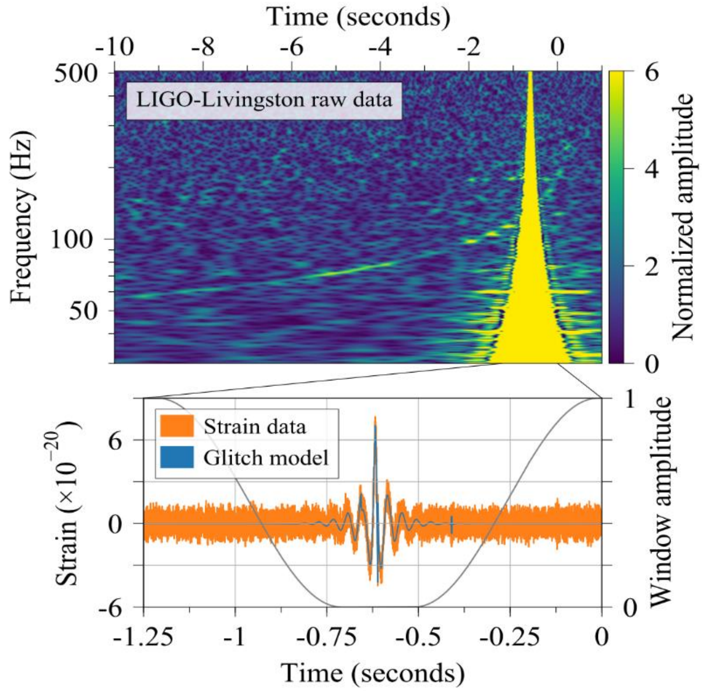

[PRD 98 084016]

[logbook entry #60547]

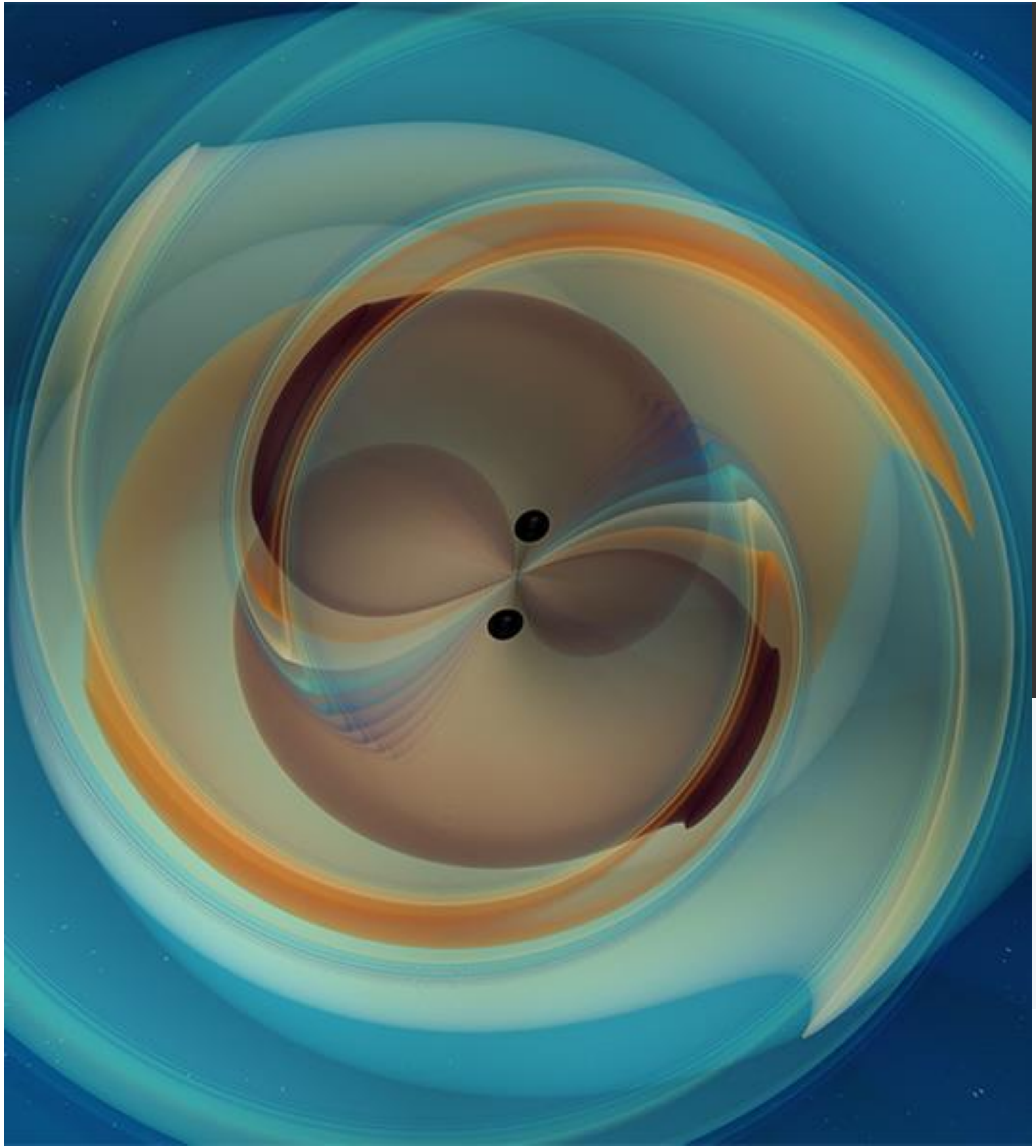

Gravitational-wave sources and searches

- Astrophysical sources of transient GW signals
- Search pipelines by the LVK collaboration
- Public alerts and multimessenger astrophysics

GW transient sources

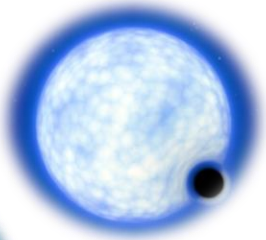

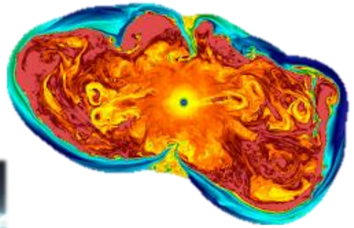

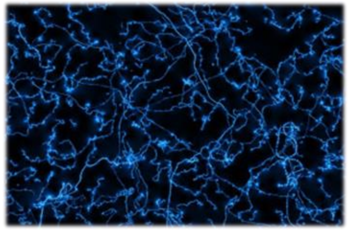

Compact Binary Coalescences

- Binary star systems made of black holes (BHs) and neutron stars (NSs): BBH, NSBH, BNS. GWTC-3
- Sub-Solar Mass (SSM) objects, MNRAS **524**, 5984 (2023)

Unmodeled or poorly modeled burst signals

- Core-collapse supernovae (CCSNe)
- Magnetar bursts
- Signals associated with fast radio bursts or gamma-ray bursts
- Cosmic strings cusps and kinks
- …

The low-latency pipeline

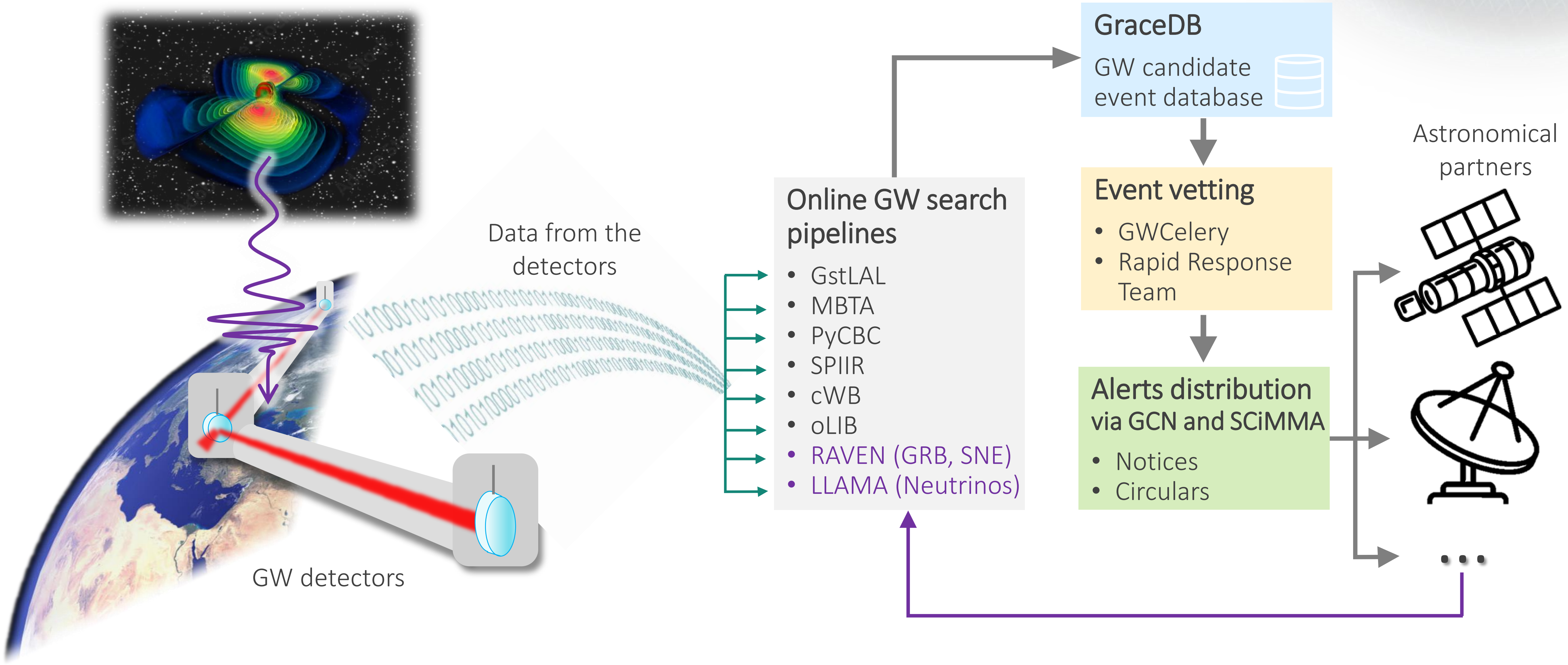

Online GW transient search pipelines

Search type	Pipeline	Description
Modeled	gstlal	Matched-filter pipeline that evaluates the ratio of the likelihood of a given signal SNR and noise residual over the same quantity for noise only data
	MBTA	Uses the matched filter technique, but splits it in two frequency bands to reduce the computational cost.
	PyCBC	Matched reweighted by imposing the consistency of the signal over various frequency bands. Time-slides method for the background estimate
	SPIIR	Applies GPU empowered summed parallel infinite impulse response (IIR) filters to approximate matched-filtering results
Unmodeled	cWB	Searches for coincidences in multiple detectors on the time-frequency data obtained with a wavelet transform
	oLIB	Time-frequency domain search over planes of constant Q factor
Coincident searches	RAVEN	Coincidences between GW events and GRBs and galactic SN alerts
	LLAMA	Combines GW triggers with High Energy Neutrino (HEN) triggers from IceCube

SNR for matched-filter based searches

Given a signal plus noise model, $\underbrace{x(t)}_{\text{detector data}} = \underbrace{n(t)}_{\text{noise}} + \underbrace{s(t)}_{\text{signal}}$, and a signal model $s(t) \approx \varrho h(t)$

with ϱ the amplitude and $h(t) = h(t; \boldsymbol{\theta})$ the waveform model ($(\boldsymbol{h}|\boldsymbol{h}) = 1$).

Optimal detection statistic: likelihood ratio, in stationary and Gaussian noise equivalent to:

$$(\boldsymbol{x}|\boldsymbol{h}) = 4\,\Re \int_0^\infty \frac{\tilde{x}(f)\tilde{h}^*(f)}{S(f)}\,df$$

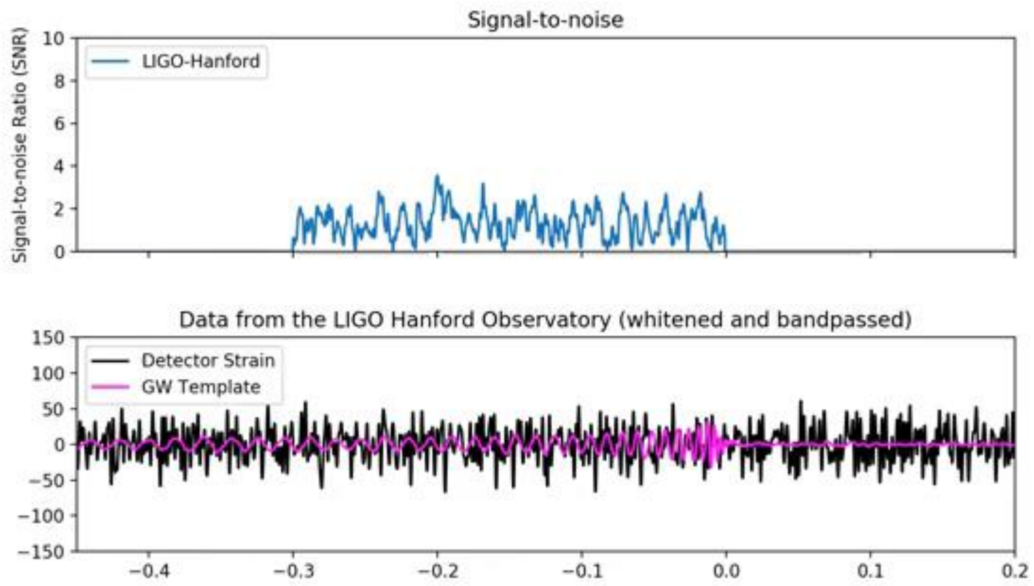

Credit Alex Nitz

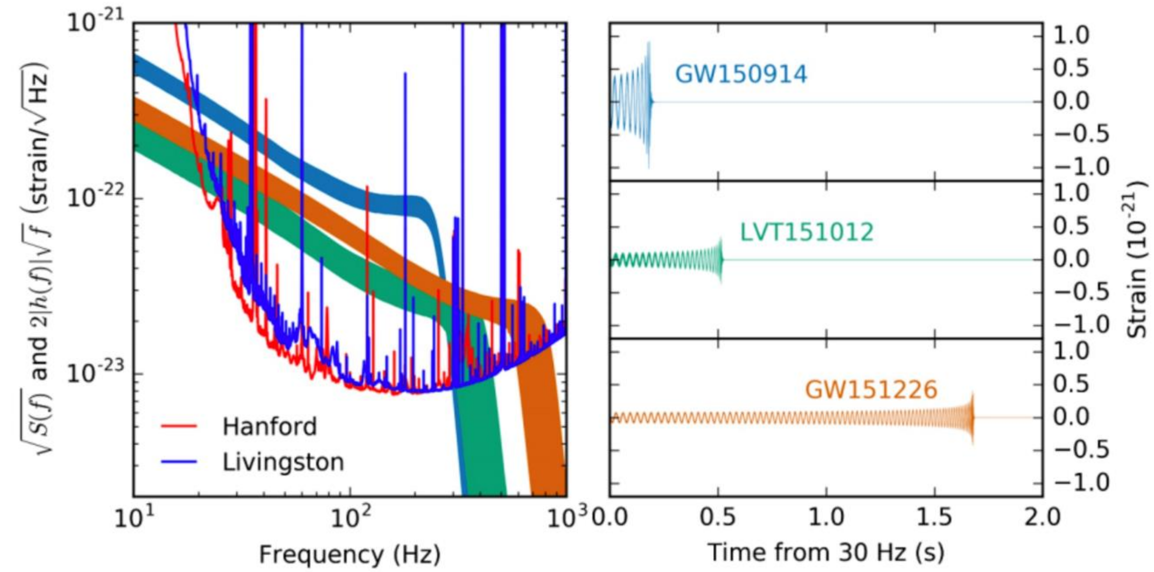

PRX 8 039903

Overview of public alerts so far

O4: 74 (85 Total - 11 Retracted), **ER15**: 2 (4 Total)

- Gravitational-Wave Candidate Event Database (**GraceDB**): https://gracedb.ligo.org/
- Gravitational Wave Open Science Center (**GWOSC**): https://gwosc.org/eventapi/html/allevents/

O4

Event ID	Possible Source (Probability)	UTC	Location	FAR
S231213ap	BBH (>99%)	Dec. 13, 2023 11:14:17 UTC		1 per 50.02 years
S231206cc	BBH (>99%)	Dec. 6, 2023 23:39:01 UTC		1 per 1.6402e+27 years
S231206ca	BBH (>99%)	Dec. 6, 2023 23:31:34 UTC		1 per 100.04 years
S231129ac	BBH (99%), Terrestrial (1%)	Nov. 29, 2023 08:17:45 UTC		1 per 1.7956 years
S231127cg	BBH (>99%)	Nov. 27, 2023 16:53:00 UTC		1 per 5.4496 years
S231123cg	BBH (>99%)	Nov. 23, 2023 13:54:30 UTC		1 per 100.04 years
S231119u	BBH (95%), Terrestrial (5%)	Nov. 19, 2023 07:52:48 UTC		2.345 per year
S231118an	BBH (74%), Terrestrial (24%), NSBH (1%)	Nov. 18, 2023 09:06:02 UTC		2.3593 per year
S231118ab	BBH (99%), Terrestrial (1%)	Nov. 18, 2023 07:14:02 UTC		1 per 1.672 years
S231118d	BBH (>99%)	Nov. 18, 2023 00:56:26 UTC		1 per 100.04 years
S231114n	BBH (>99%)	Nov. 14, 2023 04:32:11 UTC		1 per 100.04 years
S231113bw	BBH (96%), Terrestrial (4%)	Nov. 13, 2023 20:04:17 UTC		1 per 2.3265 years
S231113bb	BBH (96%), Terrestrial (4%)	Nov. 13, 2023 12:26:23 UTC		1.7663 per year
S231112ag	BBH (>99%)	Nov. 12, 2023 11:02:03 UTC		1 per 2.9871e+06 years
S231110g	BBH (97%), Terrestrial (3%)	Nov. 10, 2023 04:03:20 UTC		1 per 1.6429 years
S231108u	BBH (>99%)	Nov. 8, 2023 12:51:42 UTC		1 per 100.04 years
S231104ac	BBH (>99%)	Nov. 4, 2023 13:34:18 UTC		1 per 100.04 years
S231102w	BBH (>99%)	Nov. 2, 2023 07:17:36 UTC		1 per 5.4281e+14 years
S231030av	BNS (93%), NSBH (6%), Terrestrial (1%)	Oct. 30, 2023 12:51:11 UTC		1.3301 per year
S231029y	BBH (>99%)	Oct. 29, 2023 11:15:08 UTC		1 per 146.45 years
S231028bg	BBH (>99%)	Oct. 28, 2023 15:30:06 UTC		1 per 4.1513e+22 years
S231020bw	BBH (>99%)	Oct. 20, 2023 18:05:09 UTC		1 per 91.785 years
S231020ba	BBH (91%), NSBH (8%)	Oct. 20, 2023 14:29:47 UTC		1 per 25.01 years
S231014r	BBH (99%)	Oct. 14, 2023 04:05:32 UTC		1 per 3.0666 years
S231008ap	BBH (>99%)	Oct. 8, 2023 14:25:21 UTC		1 per 20.718 years
S231005ah	BBH (>99%)	Oct. 5, 2023 09:15:49 UTC		1 per 15.493 years
S231005j	BBH (98%), Terrestrial (2%)	Oct. 5, 2023 02:10:30 UTC		1.0148 per year
S231001aq	BBH (>99%)	Oct. 1, 2023 14:02:20 UTC		1 per 6.3814 years
S230930al	BBH (99%)	Sept. 30, 2023 11:07:30 UTC		1 per 4.2935 years
S230928cb	BBH (>99%)	Sept. 28, 2023 21:58:27 UTC		1 per 33.347 years
S230927be	BBH (>99%)	Sept. 27, 2023 15:38:32 UTC		1 per 100.04 years
S230927l	BBH (98%), Terrestrial (2%)	Sept. 27, 2023 04:37:29 UTC		1 per 2.9477 years
S230924an	BBH (>99%)	Sept. 24, 2023 12:44:53 UTC		1 per 100.04 years
S230922q	BBH (>99%)	Sept. 22, 2023 04:06:58 UTC		1 per 87.833 years
S230922g	BBH (>99%)	Sept. 22, 2023 02:03:44 UTC		1 per 1.6432e+16 years
S230920al	BBH (>99%)	Sept. 20, 2023 07:11:24 UTC		1 per 100.04 years
S230919bj	BBH (>99%)	Sept. 19, 2023 21:57:12 UTC		1 per 100.04 years
S230918aq	BNS (79%), Terrestrial (21%)	Sept. 18, 2023 11:19:41 UTC		1.7099 per year
S230914ak	BBH (99%)	Sept. 14, 2023 11:14:01 UTC		1 per 35.198 years
S230911ae	BBH (>99%)	Sept. 11, 2023 19:53:24 UTC		1 per 16769 years
S230904n	BBH (91%), Terrestrial (9%)	Sept. 4, 2023 05:10:13 UTC		1 per 14.088 years
S230831e	BBH (98%), Terrestrial (2%)	Aug. 31, 2023 01:54:14 UTC		1 per 1.6009 years
S230830b	NSBH (80%), BBH (20%)	Aug. 30, 2023 04:21:58 UTC		1 per 275.98 years
S230825k	BBH (>99%)	Aug. 25, 2023 04:13:34 UTC		1 per 13.272 years
S230824r	BBH (>99%)	Aug. 24, 2023 03:30:47 UTC		1 per 1932.8 years
S230822bm	BBH (98%), Terrestrial (2%)	Aug. 22, 2023 23:03:37 UTC		1 per 1.2262 years
S230820bq	BBH (96%), Terrestrial (4%)	Aug. 20, 2023 21:25:15 UTC		1.3351 per year
S230819ax	BBH (99%)	Aug. 19, 2023 17:19:10 UTC		1 per 3.5837 years
S230814ah	BBH (>99%)	Aug. 14, 2023 23:09:01 UTC		1 per 1.7159e+13 years
S230814r	BBH (93%), Terrestrial (7%)	Aug. 14, 2023 06:19:20 UTC		1.518 per year
S230811n	BBH (>99%)	Aug. 11, 2023 03:21:16 UTC		1 per 100.04 years
S230810af	BNS (99%)	Aug. 10, 2023 10:01:07 UTC		1 per 1.091 years
S230808i		Aug. 8, 2023 04:03:46 UTC		1 per 462.5 years
S230807f	BBH (95%), Terrestrial (5%)	Aug. 7, 2023 20:50:45 UTC		2.2538 per year
S230806ak	BBH (>99%)	Aug. 6, 2023 20:40:41 UTC		1 per 10.711 years
S230805x	BBH (>99%)	Aug. 5, 2023 03:42:49 UTC		1 per 3.4497 years
S230802aq	BBH (90%), NSBH (6%), Terrestrial (3%)	Aug. 2, 2023 11:33:59 UTC		1 per 1.4226 years
S230731an	BBH (81%), NSBH (18%)	July 31, 2023 21:53:07 UTC		1 per 100.04 years
S230729z	BBH (>99%)	July 29, 2023 08:23:17 UTC		1 per 9.3389 years
S230726a	BBH (>99%)	July 26, 2023 00:29:40 UTC		1 per 8.2692e+05 years
S230723ac	BBH (87%), Terrestrial (13%)	July 23, 2023 10:18:34 UTC		1.6821 per year
S230715bw	NSBH (91%), BBH (9%)	July 15, 2023 19:05:37 UTC		1 per 4.0401 years
S230712a	BBH (>99%)	July 12, 2023 00:53:57 UTC		1 per 9.6933e+06 years
S230709bi	BBH (>99%)	July 9, 2023 12:27:27 UTC		1 per 10.353 years
S230708cf	BBH (99%), Terrestrial (1%)	July 8, 2023 23:09:35 UTC		1 per 2.0439 years
S230708bi	BBH (>99%)	July 8, 2023 17:17:37 UTC		1 per 28.482 years
S230708z	BBH (95%), Terrestrial (5%)	July 8, 2023 07:18:59 UTC		2.2173 per year
S230708t	BBH (97%), Terrestrial (3%)	July 8, 2023 05:37:05 UTC		1.3667 per year
S230707ai	BBH (95%), Terrestrial (5%)	July 7, 2023 12:40:47 UTC		1 per 2.3021 years
S230706ah	BBH (97%), Terrestrial (3%)	July 6, 2023 10:43:33 UTC		1.3448 per year
S230704f	BBH (>99%)	July 4, 2023 02:12:11 UTC		1 per 11.255 years
S230702an	BBH (>99%)	July 2, 2023 18:54:53 UTC		1 per 20668 years
S230630bq	BBH (97%), Terrestrial (3%)	June 30, 2023 23:45:32 UTC		1 per 4.0981 years
S230630am	BBH (98%), Terrestrial (2%)	June 30, 2023 12:58:06 UTC		1 per 1.3133 years
S230628ax	BBH (>99%)	June 28, 2023 23:12:00 UTC		1 per 100.04 years
S230627c	NSBH (49%), BBH (48%), Terrestrial (3%)	June 27, 2023 01:53:37 UTC		1 per 100.04 years
S230624av	BBH (95%), Terrestrial (5%)	June 24, 2023 11:31:03 UTC		1 per 2.4372 years
S230622ba	BBH (87%), Terrestrial (13%)	June 22, 2023 14:35:36 UTC		1.6345 per year
S230609u	BBH (96%), Terrestrial (4%)	June 9, 2023 06:49:58 UTC		1 per 3.1557 years
S230608as	BBH (>99%)	June 8, 2023 20:50:47 UTC		1 per 231.43 years
S230606d	BBH (>99%)	June 6, 2023 00:43:05 UTC		1 per 2.7789 years
S230605o	BBH (99%), Terrestrial (1%)	June 5, 2023 06:53:43 UTC		1 per 7.0086 years
S230601bf	BBH (>99%)	June 1, 2023 22:41:34 UTC		1 per 1.8492e+07 years
S230529ay	NSBH (62%), BNS (31%), Terrestrial (7%)	May 29, 2023 18:15:00 UTC		1 per 160.44 years
S230524x	BNS (75%), Terrestrial (25%)	May 24, 2023 20:22:41 UTC		2.2799 per year

ER15

Event ID	Possible Source (Probability)	UTC	Location	FAR	Scan
S230522n	BBH (99%)	May 22, 2023 15:30:33 UTC		1 per 4.8908 years	H1 L1 V1
S230522a	BBH (>99%)	May 22, 2023 09:38:05 UTC		1 per 3.0614 years	H1 L1 V1
S230520ae	BBH (>99%)	May 20, 2023 22:48:42 UTC		1 per 10.354 years	H1 L1 V1
S230518h	NSBH (86%), Terrestrial (10%), BBH (4%)	May 18, 2023 12:59:08 UTC		1 per 98.463 years	H1 L1 V1

Be prepared for the next GW170817-like event!

The **Low-Latency** workflow, in brief:

A *significant* GW **signal candidate** is found by online search pipelines

A GCN alert is sent to astronomers in order to search for counterparts (EM waves or neutrinos)

The RRT provides rapid human vetting of low-latency alerts

- Foster multimessenger searches
- Trigger event validation and all downstream analyses

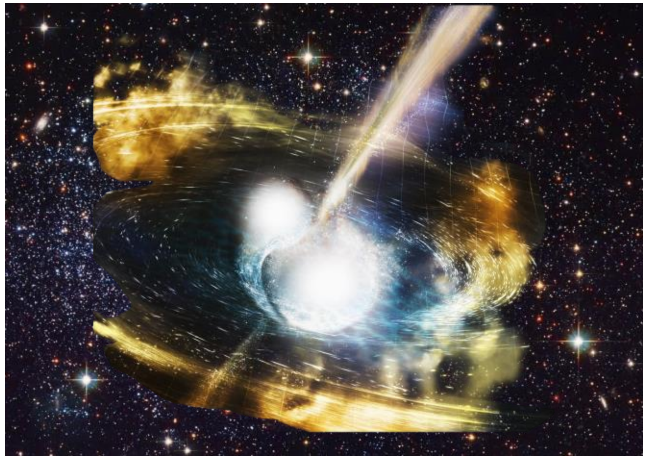

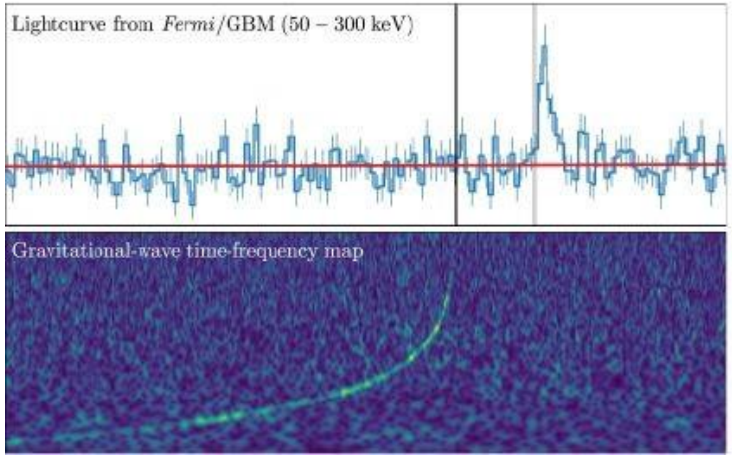

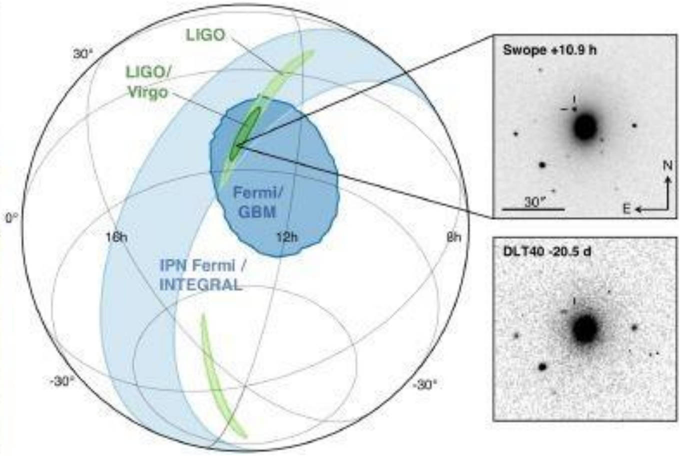

Astrophys.J.Lett. 848 (2017) 2, L12

Event triggers, Superevents and alerts

- Search pipelines produce Events, with associated **SNR** and false alarm rate (**FAR**), which are uploaded to GraceDB
- **GWCelery** clusters events, possibly from different pipelines, on the basis of coalescence time for modeled searches, and trigger time for unmodeled searches, to Superevents
- The **preferred event** is identified on the base of FAR, SNR and search kind.

Alerts:

- **Low-significance:** preferred event FAR is < 2 per day; a "preliminary alert" is sent out but no human vetting
- **Significant event:** FAR < 1 per month* for modeled CBC candidates and < 1 per year* for unmodeled burst candidates.

Alert timeline

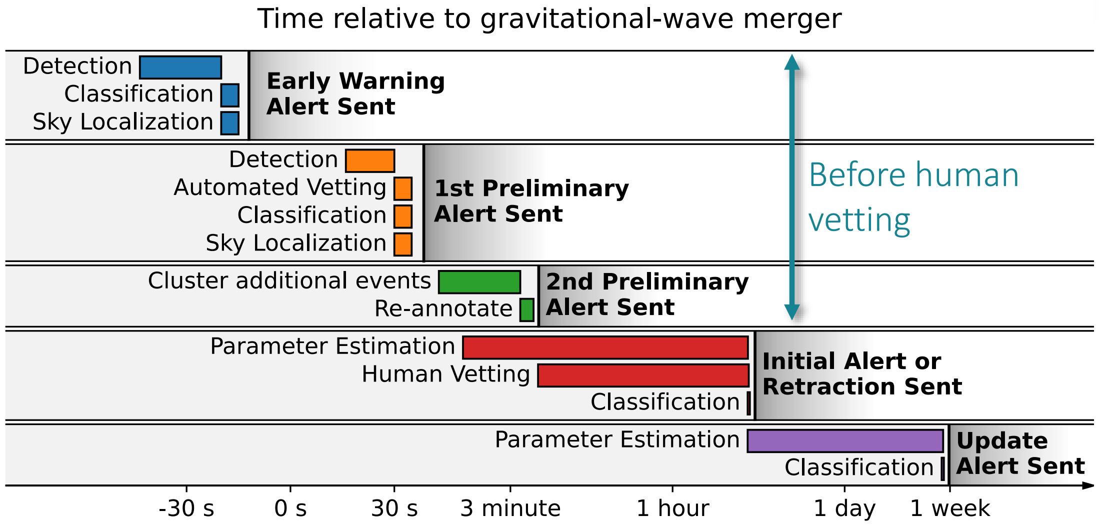

LVK Public Alerts Open Guide

* **Alert threshold after trials factor:** to account for the trials factor from the different searches with statistically independent FARs, the event thresholds are corrected to 1 per 6 months and 1 per 4 years for CBC and bursts respectively.

The rapid response team and human vetting timeline

Rapid Response Team (RRT)

A joint LVK effort to provide human vetting to event alerts:

- Foster multimessenger searches
- Vet candidates with evidence of noise artefacts

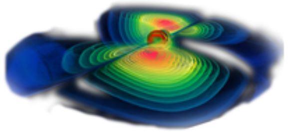

Three tier system

- Level-0 shifters, online 24/7 over three shifts per day (almost 300 participants total)
- Level-1 experts of data quality and all the parts of the low-latency pipeline
- Level-2: all the above, called for vetting **high profile events.**

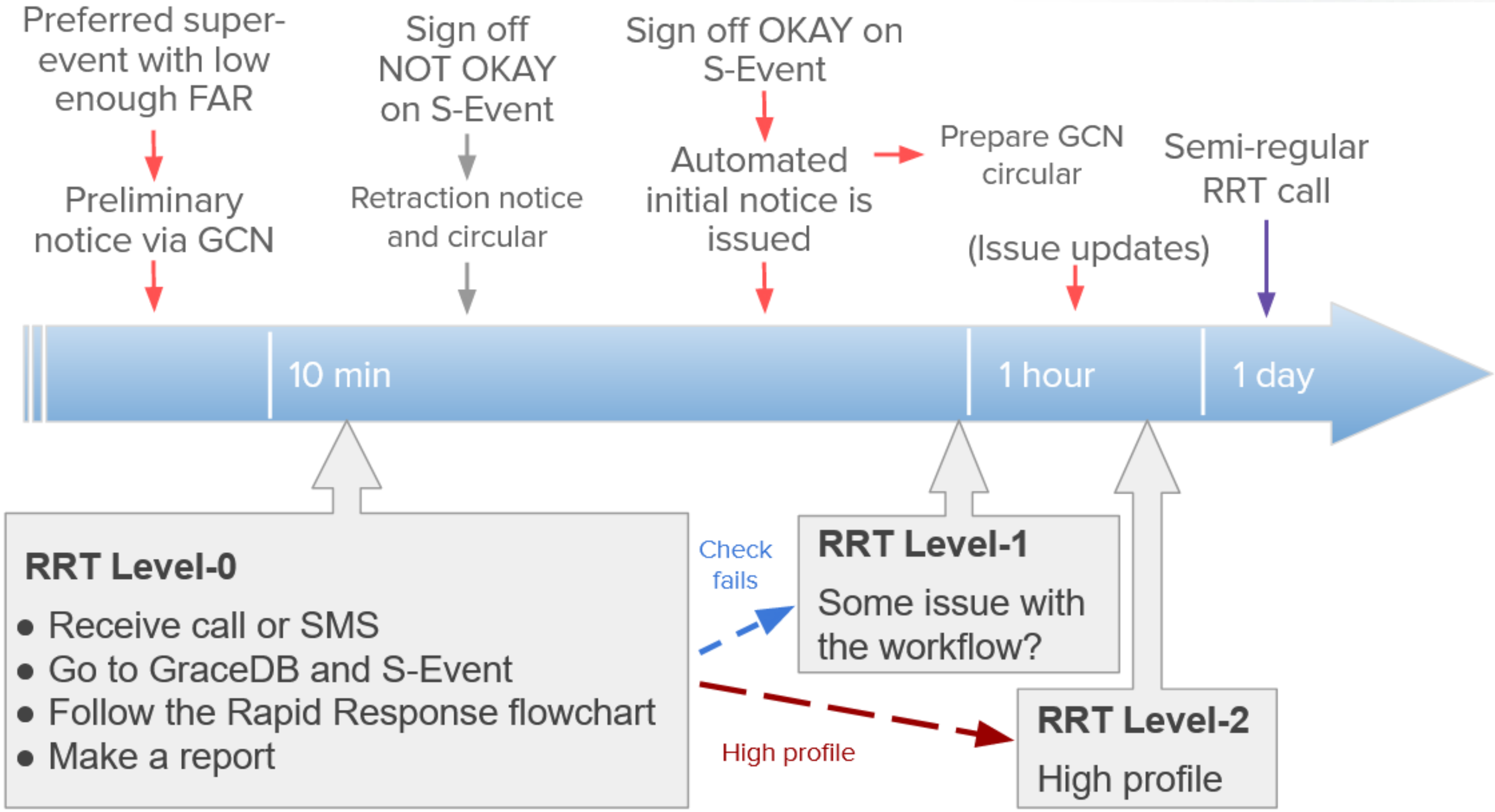

Notices and circulars, content of a GCN alert

```
////////////////////////////////////////////////////////////////////////
TITLE:            GCN/LVC NOTICE
NOTICE_DATE:      Thu 18 May 23 13:38:21 UT
NOTICE_TYPE:      LVC Preliminary
TRIGGER_NUM:      S230518h
TRIGGER_DATE:     20082 TJD;   138 DOY;   2023/05/18 (yyyy/mm/dd)
TRIGGER_TIME:     46748.000000 SOD {12:59:08.000000} UT
SEQUENCE_NUM:     1
GROUP_TYPE:       1 = CBC
SEARCH_TYPE:      1 = AllSky
PIPELINE_TYPE:    15 = pycbc
FAR:              3.219e-10 [Hz]  (one per 35957.2 days)  (one per 98.51 years)
PROB_NS:          1.00 [range is 0.0-1.0]
PROB_REMNANT:     0.00 [range is 0.0-1.0]
PROB_BNS:         0.00 [range is 0.0-1.0]
PROB_NSBH:        0.86 [range is 0.0-1.0]
PROB_BBH:         0.03 [range is 0.0-1.0]
PROB_MassGap:     -1 [range is 0.0-1.0]   VALUE NOT ASSIGNED!
PROB_TERRES:      0.09 [range is 0.0-1.0]
TRIGGER_ID:       0x10
MISC:             0x189A003
SKYMAP_FITS_URL:
https://gracedb.ligo.org/api/superevents/S230518h/files/bayestar.multiorder.fits
EVENTPAGE_URL:    https://gracedb.ligo.org/superevents/S230518h/view/
COMMENTS:         LVC Preliminary Trigger Alert.
COMMENTS:         This event is an OpenAlert.
COMMENTS:         LIGO-Hanford Observatory contributed to this candidate event.
COMMENTS:         LIGO-Livingston Observatory contributed to this candidate event
```

- Trigger time
- Search type
- Source classification
- EM-bright properties
  More details in the EM-follow guide
- Sky localization

GCN Circular 33813

Subject LIGO/Virgo/KAGRA S230518h: Identification of a GW compact binary merger candidate
Date 2023-05-18T14:06:25Z (5 months ago)
From f.di-renzo@ip2i.in2p3.fr

The LIGO Scientific Collaboration, the Virgo Collaboration, and the KAGRA Collaboration report:

We identified the compact binary merger candidate S230518h during real-time processing of data from LIGO Hanford Observatory (H1) and LIGO Livingston Observatory (L1) at 2023-05-18 12:59:08.167 UTC (GPS time: 1368449966.167). The candidate was found by the PyCBC Live [1], GstLAL [2], and MBTAOnline [5] analysis pipelines.

The LIGO detectors are currently operating in an "engineering run" mode prior to the start of the O4 observing run. The data being collected at the time of this candidate is believed to be of good quality based on preliminary checks, but requires further investigation. A decision was made to alert the community promptly, with this caveat, due to the potential significance of this candidate.

S230518h is an event of interest because its false alarm rate, as estimated by the online analysis, is 3.2e-10 Hz, or about one in 98 years. The event's properties can be found at this URL:
https://gracedb.ligo.org/superevents/S230518h

The classification of the GW signal, in order of descending probability, is NSBH (86%), Terrestrial (10%), BBH (4%), or BNS (<1%).

Assuming the candidate is astrophysical in origin, the probability that the lighter compact object is consistent with a neutron star mass (HasNS) is >99%. [3] Using the masses and spins inferred from the signal, the probability of matter outside the final compact object (HasRemnant) is < 1%. Both HasNS and HasRemnant consider the support of several neutron star equations of state. The probability that any one of the binary components lie between 3 to 5 solar mass (HasMassgap) is < 1%.

One sky map is available at this time and can be retrieved from the GraceDB event page:
* bayestar.multiorder.fits, an initial localization generated by BAYESTAR [4], distributed via GCN Notice about 39 minutes after the candidate event time.

For the bayestar.multiorder.fits sky map, the 90% credible region is 1002 deg2. Marginalized over the whole sky, the a posteriori luminosity distance estimate is 276 +/- 79 Mpc (a posteriori mean +/- standard deviation).

GCN Circular 33813

O4 alert latency and event distribution

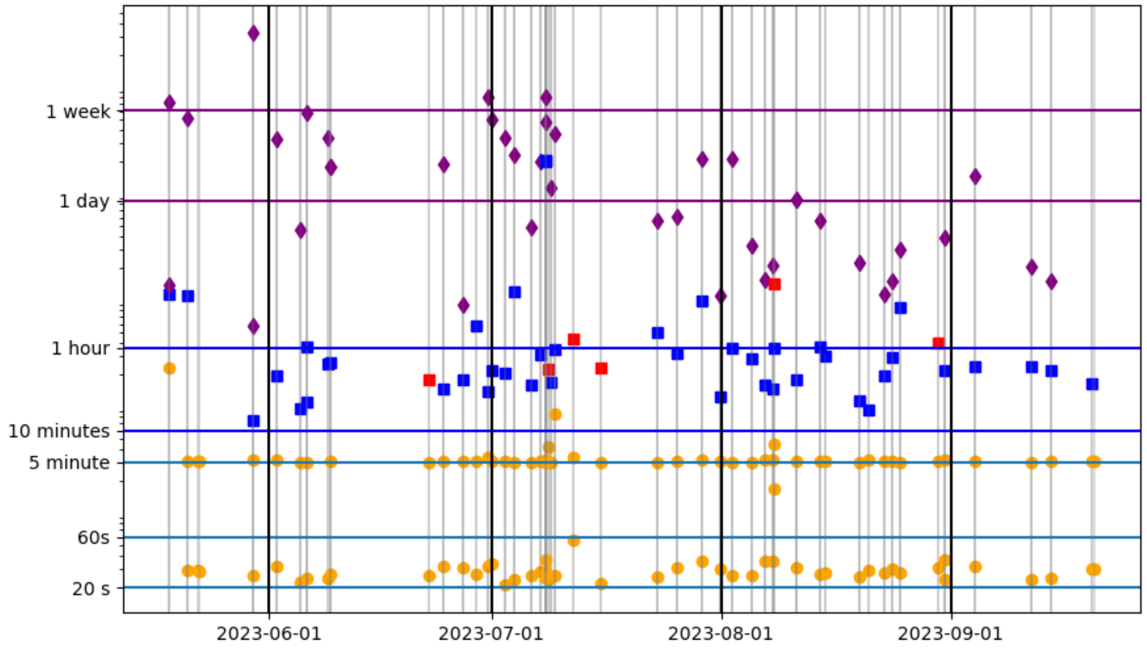

Image credit: Roberto De Pietri

- Preliminary notices
- Initial notice (38')
- Retraction notice (38')
- Update notices

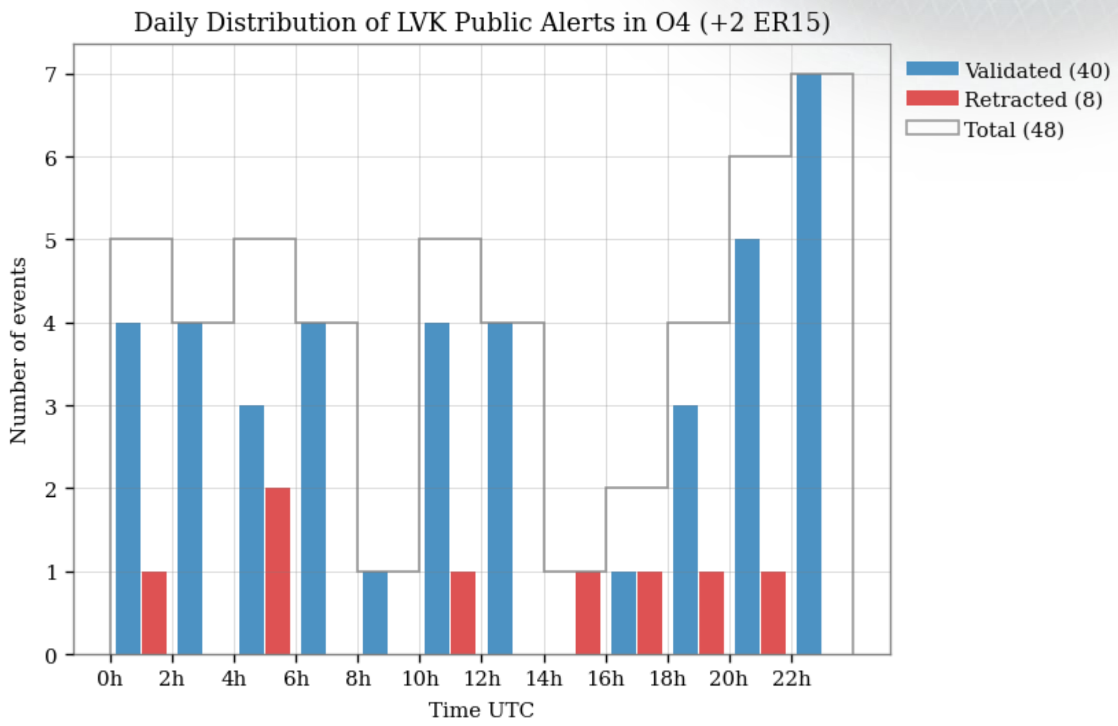

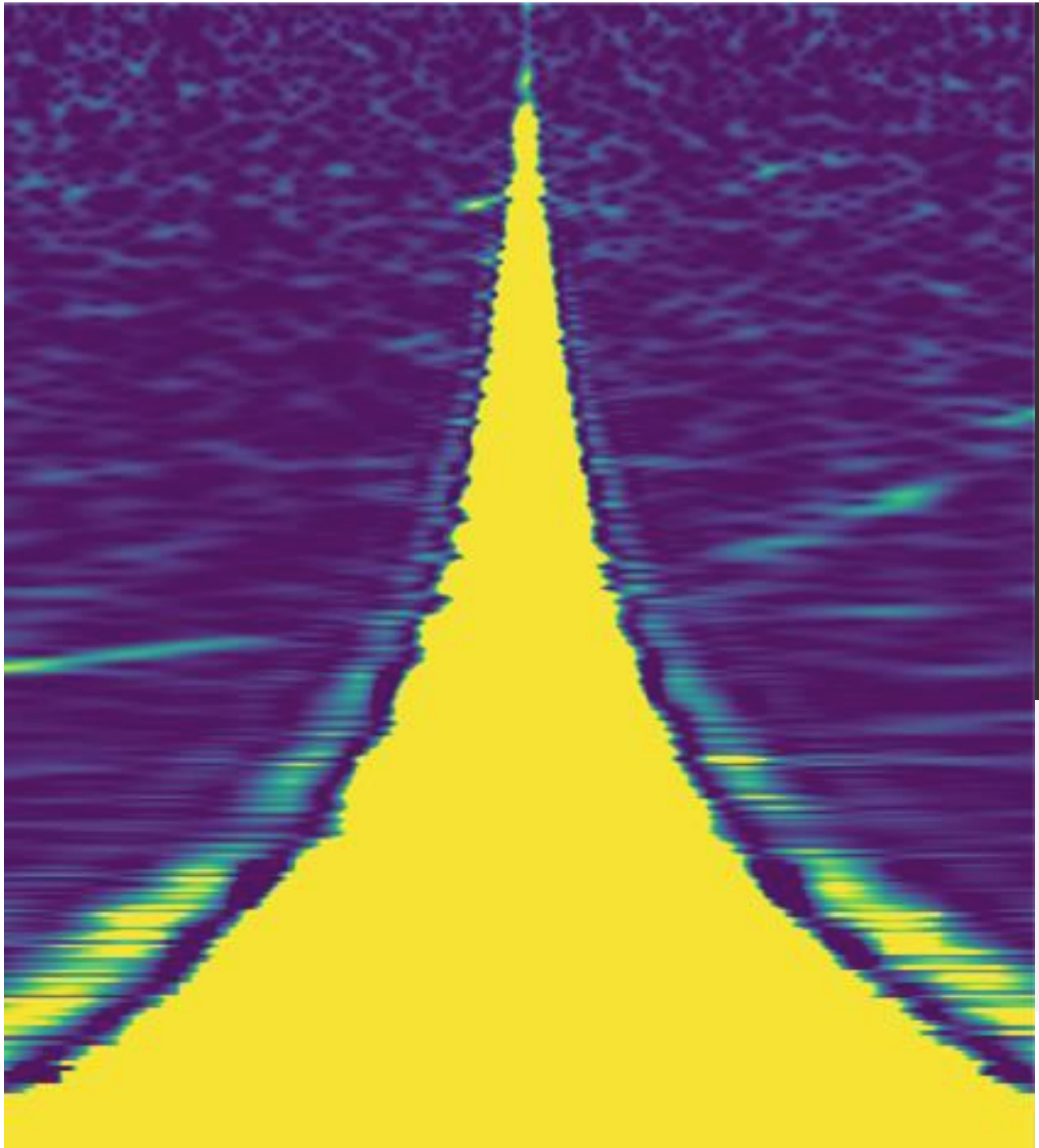

Event validation and Data Quality

- Event validation
- The Data Quality Report framework
- Noise artifact mitigation

Data processing overview: from detectors to publications

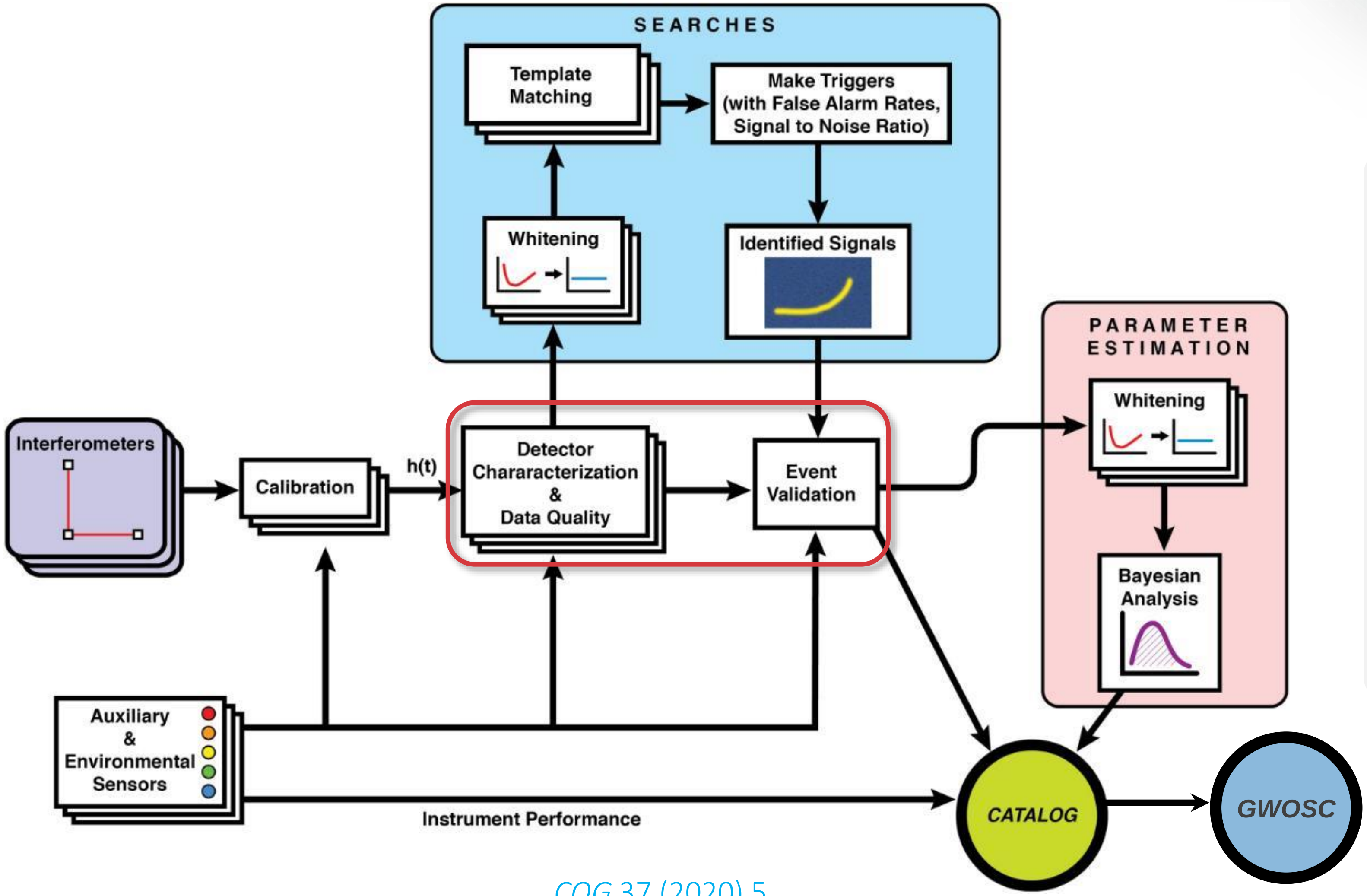

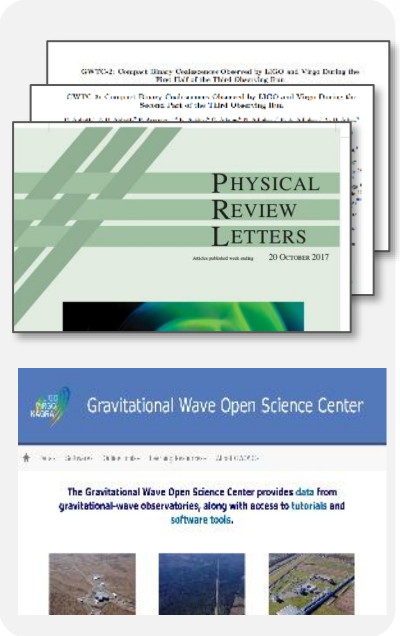

CQG 37 (2020) 5

The validation of gravitational-wave events

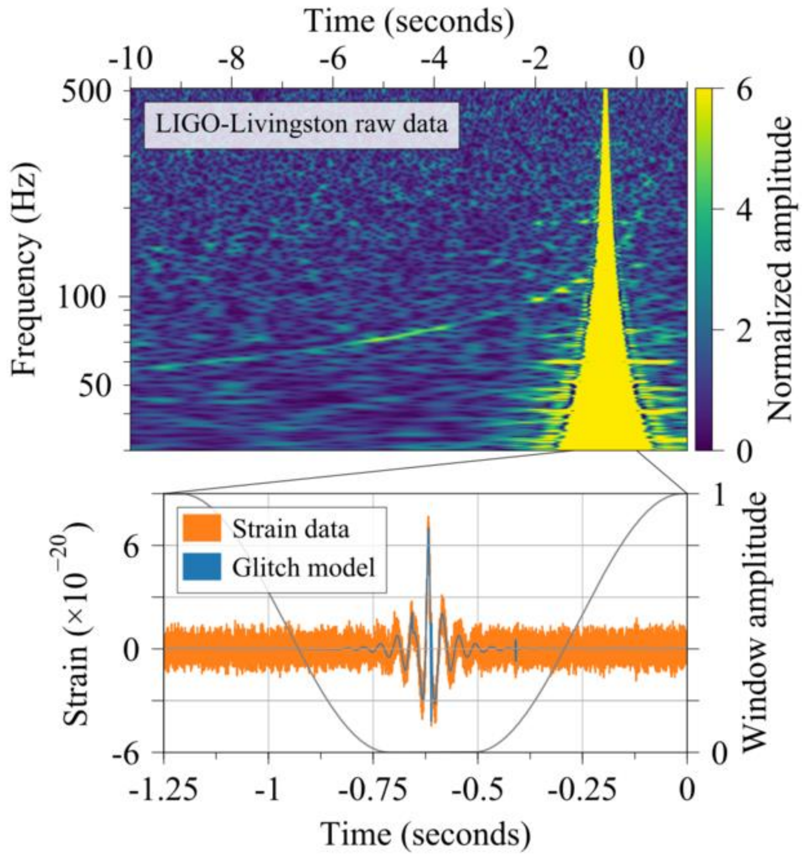

PRD 98, 084016 (2018)

- **Event validation** consists of a set of procedures to verify if **data quality (DQ) issues**, such as instrumental artifacts, environmental disturbances, or anomalies in the search pipelines, can impact the analysis results and **decrease the confidence of a detection**;
- It is applied to all gravitational-wave transient **candidate events** found by both *online* and *offline* search pipelines;
- Typically, candidate events undergo **two stages of validation**:
  - **Prompt validation (RRT, online triggers only)**:

    Accompanies every public alerts and is typically completed within $\mathcal{O}(10 \text{ min})$ from the data acquisition. It has the role to **vet** an event trigger if there is evidence of terrestrial origin or other severe DQ issues;
  - **Offline validation (all)**:

    Completed as a final check before publication for all events found by online and/or offline pipelines. The typical timescale is days or even months after the time of the event.

The Data Quality Report framework

Schematics of the Virgo O3 DQR architecture, from CQG **40**, 185006 (2023)

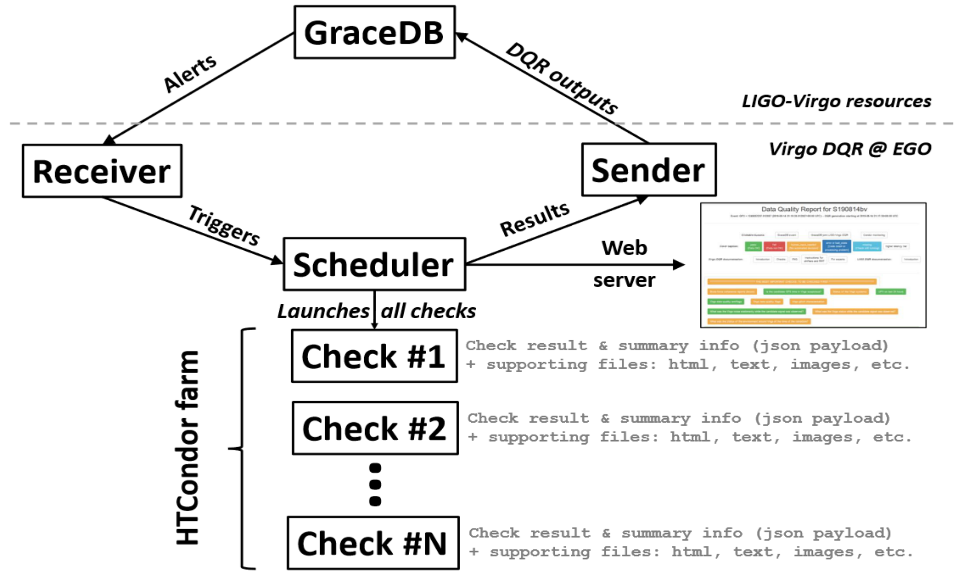

Snapshot from the "LIGO DQR" (credit Areeda, Davis)

H1 result: Pass Observing

Task	IFO	Status	P-value	Result
glitchaverage	H1	Done	0.14768264	Pass
stationarity	H1	Done	0.375	Pass
pemcheck	H1	Done	0.51362564	Pass
rayleigh	H1	Done	0.609375	Pass
omega_overlap	H1	Done	0.6546039	Pass
glitchfind	H1	Done	0.91762616	Pass
gspynettree	H1	Done	0.9683	Pass

- A **Data Quality Report** (DQR) is a framework developed by LIGO and Virgo consisting in a set of DQ checks;
- Two parallel implementations: "Virgo DQR" and "LIGO DQR"
- It is automatically prompted after each gravitational-wave candidate trigger with false alarm rate (FAR) of $1/\mathrm{day}$ is being generated on GraceDB;
- The results are uploaded back to GraceDB and used by the **Rapid Response Team** to validate or vet the associated event, and afterwards for the final event validation.

Table: Performance of Virgo DQR during O3b, from CQG **40**, 185006 (2023)

Operation	Time taken [s]		
	Median	Mean	95^{th} percentile
Data acquired → Candidate on GraceDB	52	166	331
Candidate on GraceDB → `LVAlert` trigger	4	4	11
`LVAlert` trigger → Virgo `DQR` configured	331	339	383
Virgo `DQR` configured → Virgo `DQR` started	8	10	21

Operation	Time from start [s]		
	Median	Mean	95^{th} percentile
Quick key checks	374	383	619
Adding `Omicron` trigger distributions	868	816	935
Adding full `Omicron` scans	1740	2159	4690
End	5185	4954	6330

Prompt event validation of low-latency alerts

Example of **Virgo DMS**. From Virgo logbook entry #56363 (NOT a candidate event) VIR-0191A-12

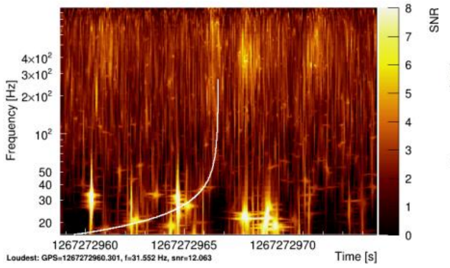

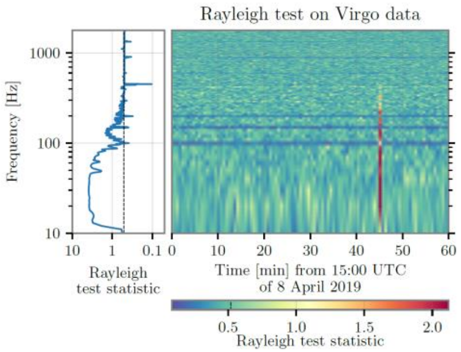

CQG **40** 185005

166.88	SDB1_LC_TZ_fb (0.24)	SDB1_LC_TZ_corr (0.24)	SDB1_LC_TZ_err (0.24)	SDB1_LC_TZ (0.24)	SDB1_LC_COIL_FL_V (0.24)
167.00	SDB1_LC_TZ_fb (0.32)	SDB1_LC_TZ_corr (0.32)	SDB1_LC_COIL_FL_V (0.32)	SDB1_LC_COIL_BL_V (0.32)	SDB1_LC_COIL_BR_V (0.32)
167.12	SDB1_LC_COIL_FR_V (0.45)	SDB1_LC_COIL_BL_V (0.45)	SDB1_LC_COIL_FL_V (0.45)	SDB1_LC_COIL_BR_V (0.45)	SDB1_LC_TZ_err (0.45)

- This stage has the role to **vet those event triggers with severe noise contamination**, for which an astrophysical origin should be excluded;
- Otherwise, it serves to enforce the confidence in the event type and **sky-localization** to support multimessenger follow-up.
- The **main DQ checks** based on the DQR are:
  - Operational **status of the detector** and its subsystems at the time of the trigger and around it;
  - Scan of the **main DQ flags**: h_{rec} correctly computed, detector observational intent and working condition, injections of spurious signals, etc.
  - **Noise characterization**: stationarity and Gaussianity, including the presence of glitches and their distribution; correlation with auxiliary channels; status of the environment, etc.

Final validation before publications

- **Every LVK publications** (catalogs and exceptional events) undergo a final, comprehensive validation procedure before data analysis reruns;
- This includes all the events found online and pre-validated and those found by offline pipelines;
- An event validation team is in charge of this procedure. Each event requires $\mathcal{O}(1\ \text{hour})$ per person involved if no DQ issue is found;
- The goal is to assess whether the parameter estimation of the astrophysical source can be affected by noise artifacts; [*CQG* 35 (2018) 15, 155017]
- If no DQ issue is found, the candidate event is considered validated;
- For those events where noise artifacts are found in the vicinity of the putative GW signal, or even overlapping with it, a procedure of **noise mitigation** is implemented. This requires additional time and person power.

Glitch: 90% credible region 137 deg^2

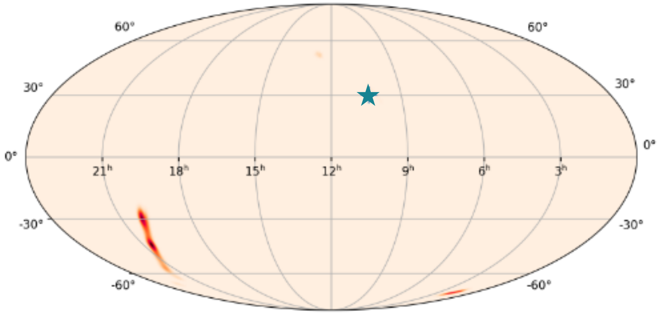

No glitch: 90% credible region 8 deg^2

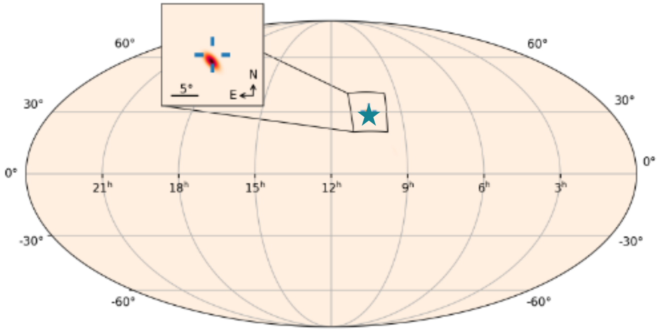

Effect on sky-localization of a blip glitch 30 ms after a GW150914-like event. [PRD 105 (2022) 103021]

Noise artifacts mitigation of gravitational-wave detector data

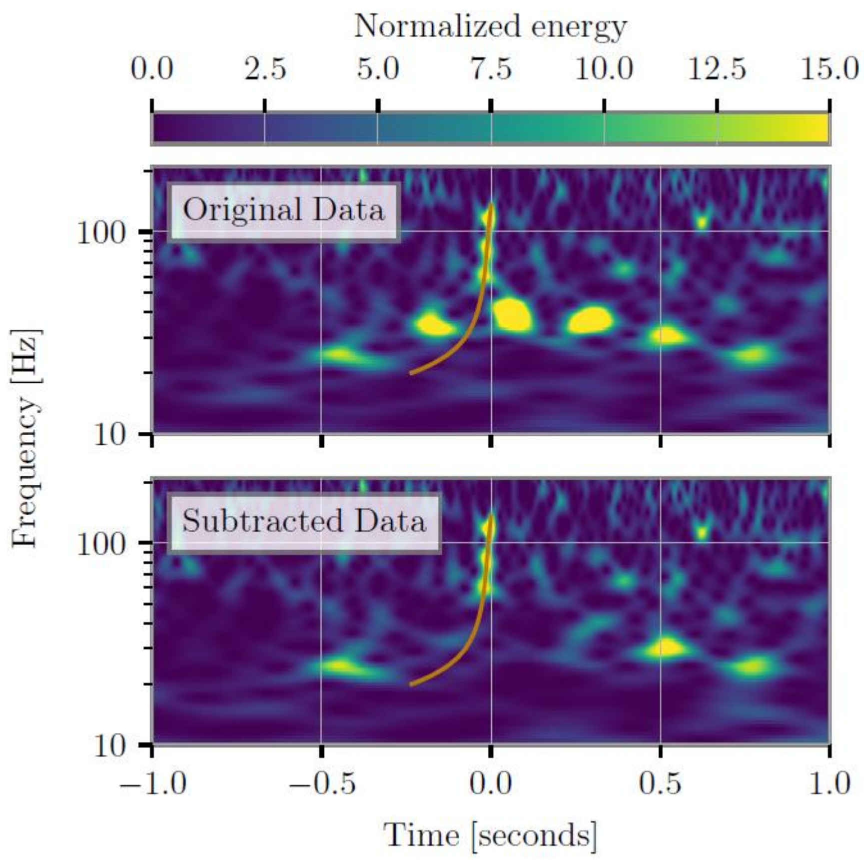

[PRX 11, 021053 (2021)](#)

- Applied to those events flagged to have DQ issues: transient noise, namely **glitches**, superimposing the putative astrophysical signal (orange curve);
- Metric based on the PSD variation to assess the extent of each non-stationary region identified [CQG 37 (2020) 21];
- Deglitched frames mostly produced with BayesWave pipeline [CQG 32 (2015) 13];
- Assessment of subtraction by means of the previous stationarity metric. Parameter Estimation comparison tests to check for bias and systematics;
- **16 events** (≈20%) required glitch subtraction during O3. This process involves lots of human input and slows down downstream analyses.

Summary of the O4 run so far

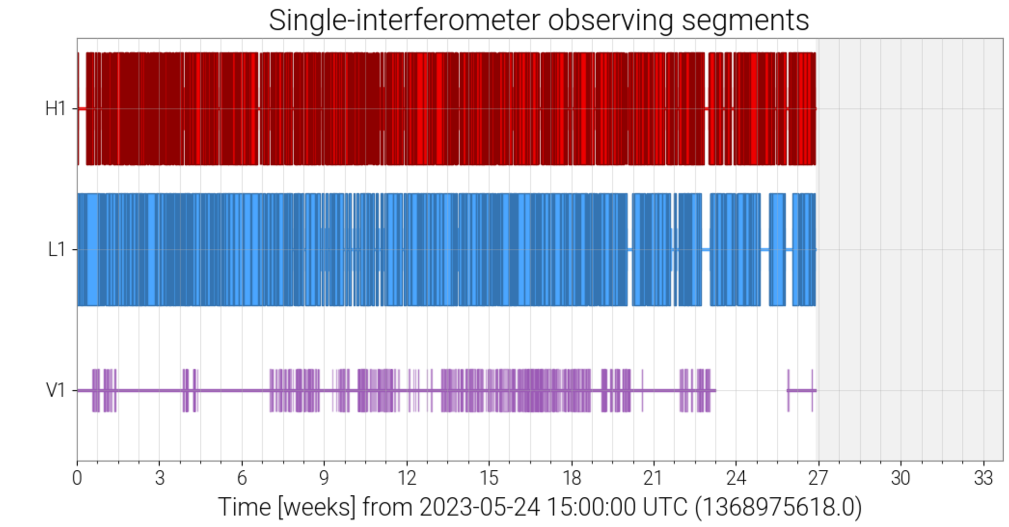

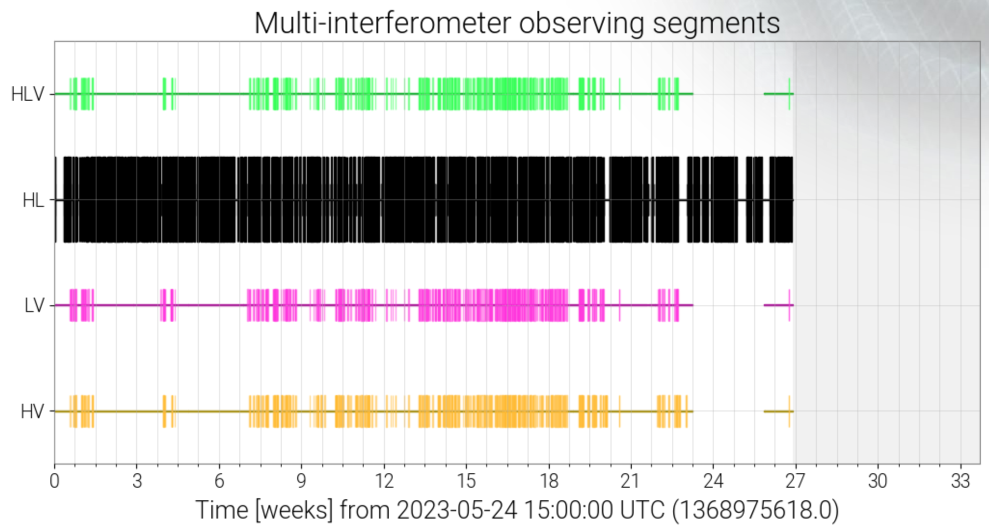

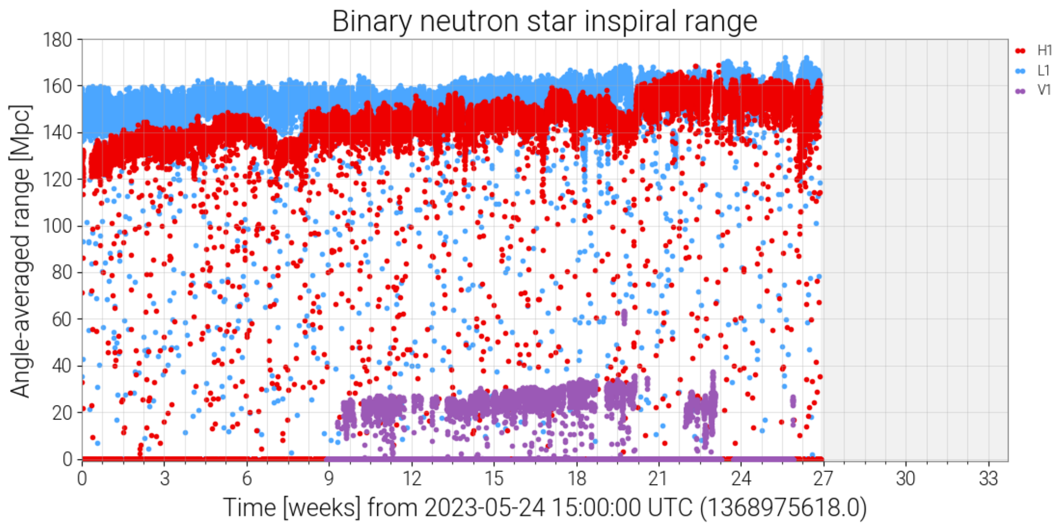

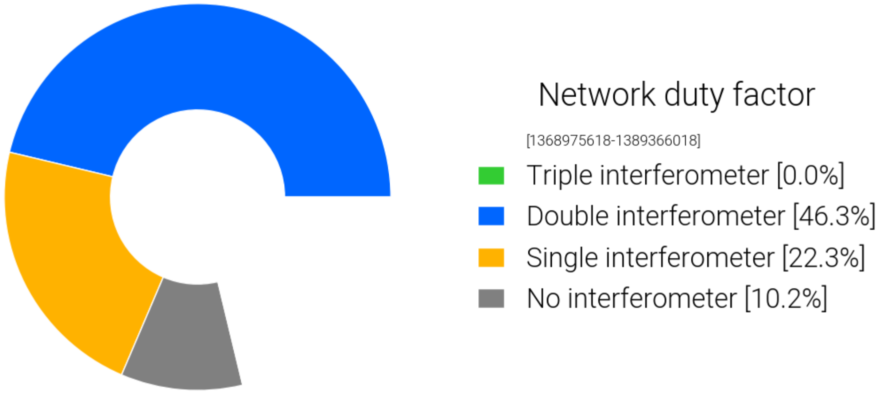

Remain up to date on the GWOSC detector status Summary

Conclusions

- Advanced GW detectors have improved their performance, beating the standard quantum noise limitations, and they are approaching their design sensitivity;
- O4 is off of a good start:
  - Same number of detections achieved in only 6 months and with 2 detectors as in the 11 months of O3, with three detectors, online+offline!
  - Improved rapid response infrastructure and DQ checks to deliver timely and trustworthy alerts
  - Virgo has prolonged the commissioning of the new optical configuration.
    It is expected to join O4 in March 2024. This will lead to an increased rate of events
- Event validation is an integrating part of GW data analysis with the role of enforcing the confidence in the astrophysical origin of a transient signal detected by search pipelines, and the reliability of the source parameter estimation results;
- Cooperation inside LVK is paramount to maintaining the rapid response infrastructure: 300 participants allover the globe, directly involved in GW transient searches.

Thanks for the attention!

The Einstein Equation

or ''spacetime tells matter how to move, matter tells spacetime how to curve'.' John A. Wheeler.

In general relativity gravity is described by the curvature of spacetime :

Curvature of spacetime →

$$G_{\mu\nu} = \frac{8\pi G}{c^4} T_{\mu\nu}$$

← Distribution of mass/energy

← Some constants

Linearized theory: $g_{\mu\nu} \approx \eta_{\mu\nu} + h_{\mu\nu}$. General relativity admits propagating, wave-like solutions. In the *Lorentz gauge*:

D'Alambertian (wave operator) →

$$\Box h_{\mu\nu} = -\frac{16\pi G}{c^4} T_{\mu\nu} + \mathcal{O}(h^2)$$

Gravitational Waves (GW): *ripples* in spacetime, produced by accelerating masses, which propagates in spacetime at speed c.

Production and free propagation of GWs

Production: accelerating mass densities:

$$h_{\mu\nu} \approx \frac{2}{r}\frac{G}{c^4}\ddot{I}_{\mu\nu}$$

Second derivative of quadrupole moment

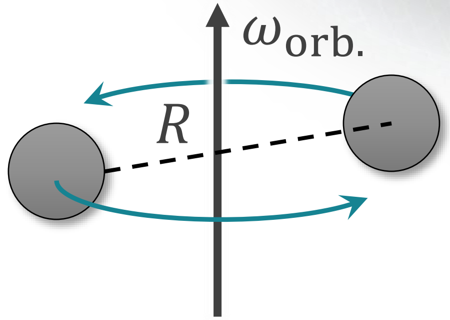

E.g.: for an orbiting binary system $I \approx MR^2, \ddot{I} \approx 4MR^2\omega_{\text{orb.}}^2$,

$$h \approx \frac{8G}{c^4}\frac{M}{r}R^2\omega_{\text{orb.}}^2 \approx \frac{8G}{c^2}\frac{M}{r}\left(\frac{v}{c}\right)^2 \sim \mathbf{10^{-21}}$$

Free propagation along "z-axis" in vacuum ($T_{\mu\nu} = 0$):

$$\Box h_{\mu\nu} = 0 \implies h_{\mu\nu}(t,z) = h_{\mu\nu}e^{i(kz-\omega t)} \quad \text{with} \quad \omega/c = k$$

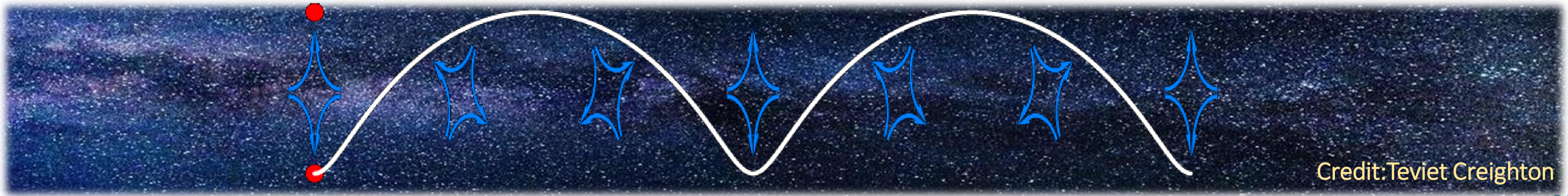

GW interaction in the TT frame

or how to exploit gauge freedom in our favor.

Transverse Traceless gauge, convenient to represent GW propagating degrees of freedom:

$$h_{ij}^{\mathrm{TT}}(t,z) = \begin{pmatrix} h_+ & h_\times & 0 \\ h_\times & -h_+ & 0 \\ 0 & 0 & 0 \end{pmatrix} \cos[\omega(t - z/c)]$$

- In this gauge, GWs are transverse and traceless (TT): h_+ and $h_\times$ d.o.f.
- Objects initially at rest **remain at rest**, even after the arrival of the wave. That is, they are "free falling":

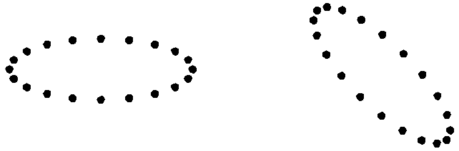

Geodesic equation →

$$\left.\frac{d^2x^i}{d\tau^2}\right|_{\tau=0} = -\left[\Gamma^i_{\nu\rho}(x)\frac{dx^\nu}{d\tau}\frac{dx^\rho}{d\tau}\right]\bigg|_{\tau=0} = \left[\Gamma^i_{00}\left(\frac{dx^0}{d\tau}\right)^2\right]\bigg|_{\tau=0} = 0$$

Because, in this gauge, the Christoffel symbol $\Gamma^i_{00} = \frac{1}{2}(2\partial_0 h_{0i} - \partial_i h_{00}) = 0$.

Only a non-gravitational force can cause a mass to change its coordinates.

Light travel time through the detector (TT gauge)

Suspended (test) masses can be considered free in the horizontal plane ($z = 0$).

We study in the TT gauge the propagation of light between them. Along one arm, the effect of a $+$ wave:

$$ds^2 = -c^2dt^2 + [1 + h_+]dx^2 = 0$$

← Light-like interval

$$\int dt = \frac{1}{c}\int \sqrt{1 + h_+}\, dx \approx \frac{1}{c}\int 1 + \frac{1}{2}h_+ dx$$

$$\Delta t \approx h_+ L/2c$$

Round trip back to beam-splitter:

$$\Delta t_x \approx h_+ L/c \qquad (\Delta t_y \approx -h_+ L/c\,)$$

Opposite sign along y

Difference between x and y round-trip times:

$$\boldsymbol{\Delta\tau = \Delta t_x - \Delta t_y \approx 2h_+ L/c \qquad (\Delta\phi \approx 2h_+ L\, 2\pi/\lambda)}$$

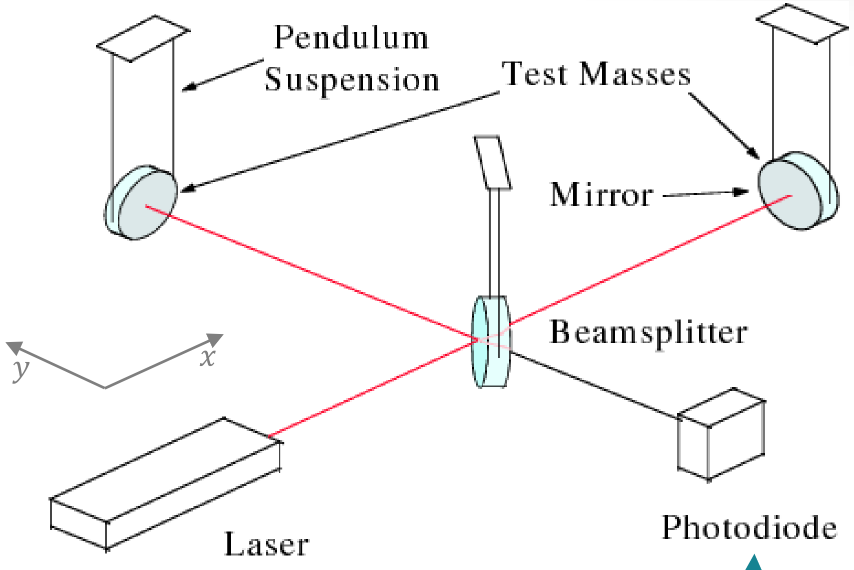

Workflow investigation of a "transient signal"

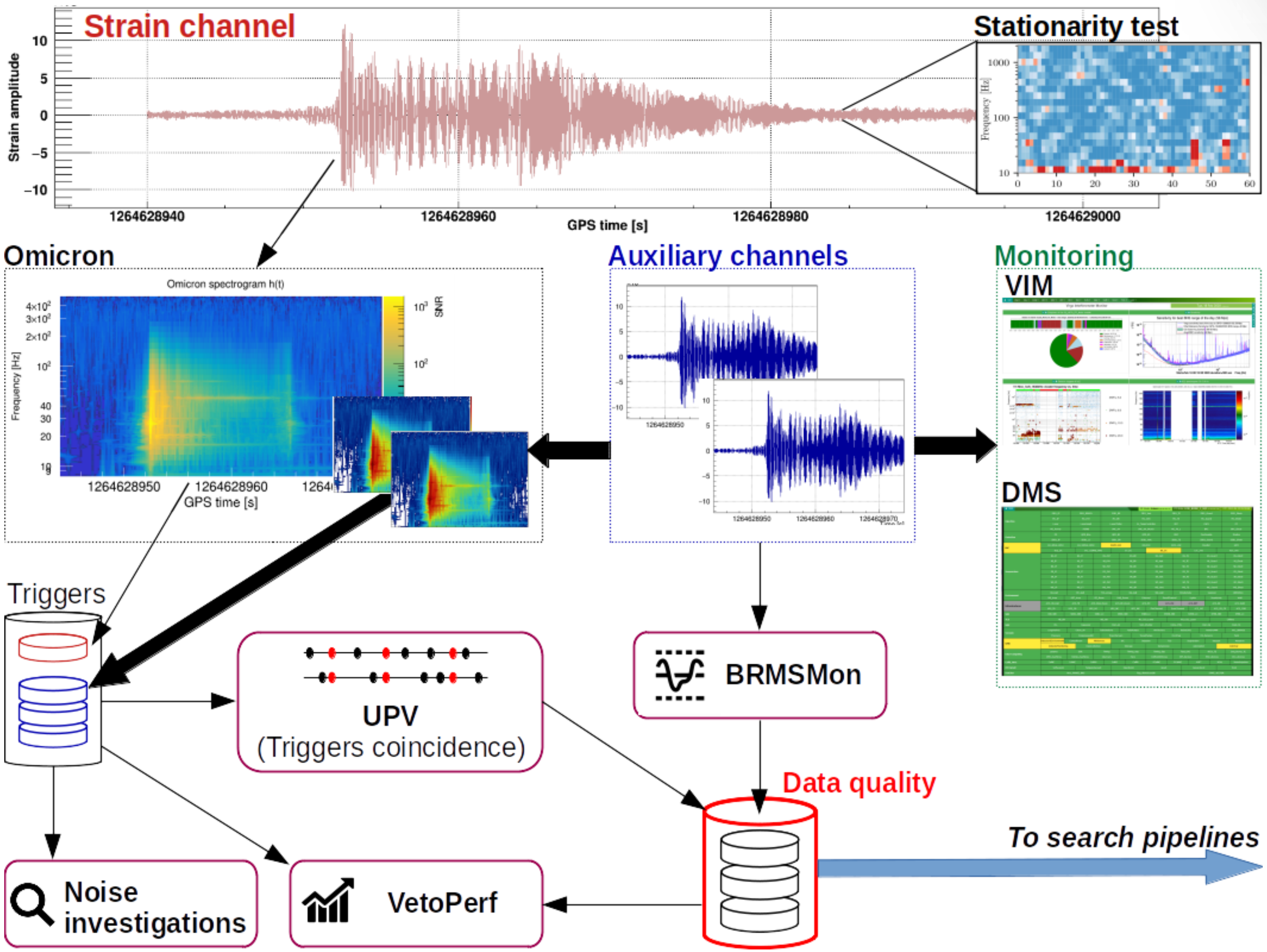

Sensitivity improvements and event rate vs time

A sensitivity range improvement of $50 \div 200\%$ implies an increase in observed volume of $2 \div 4$ times, and an equal increase in detected events.

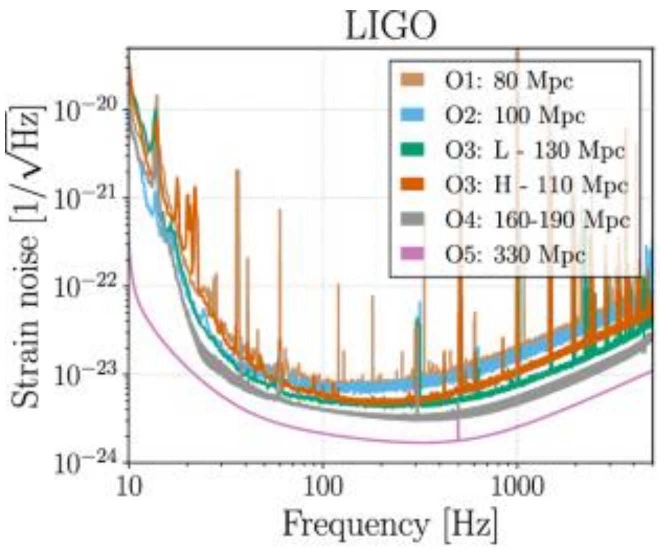

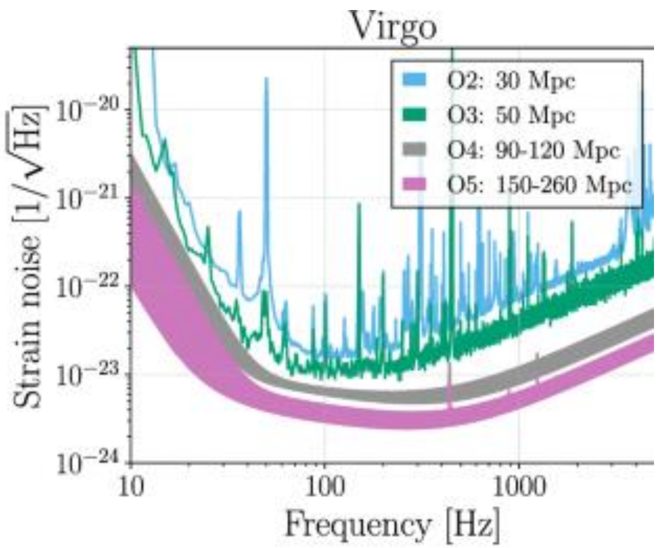

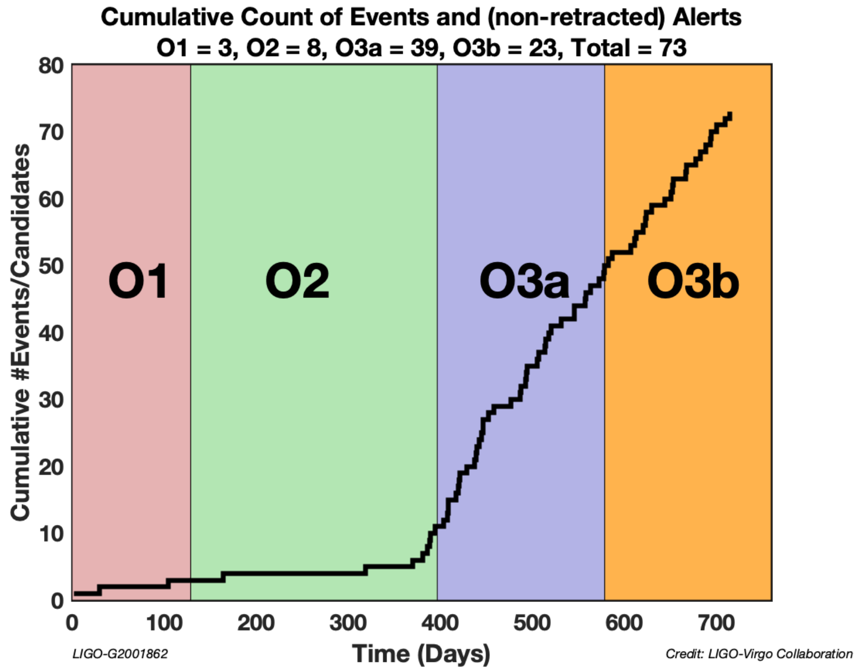

Living Rev.Rel. 23 (2020) 1, 3

LIGO-G2001862

LVK observing run plans

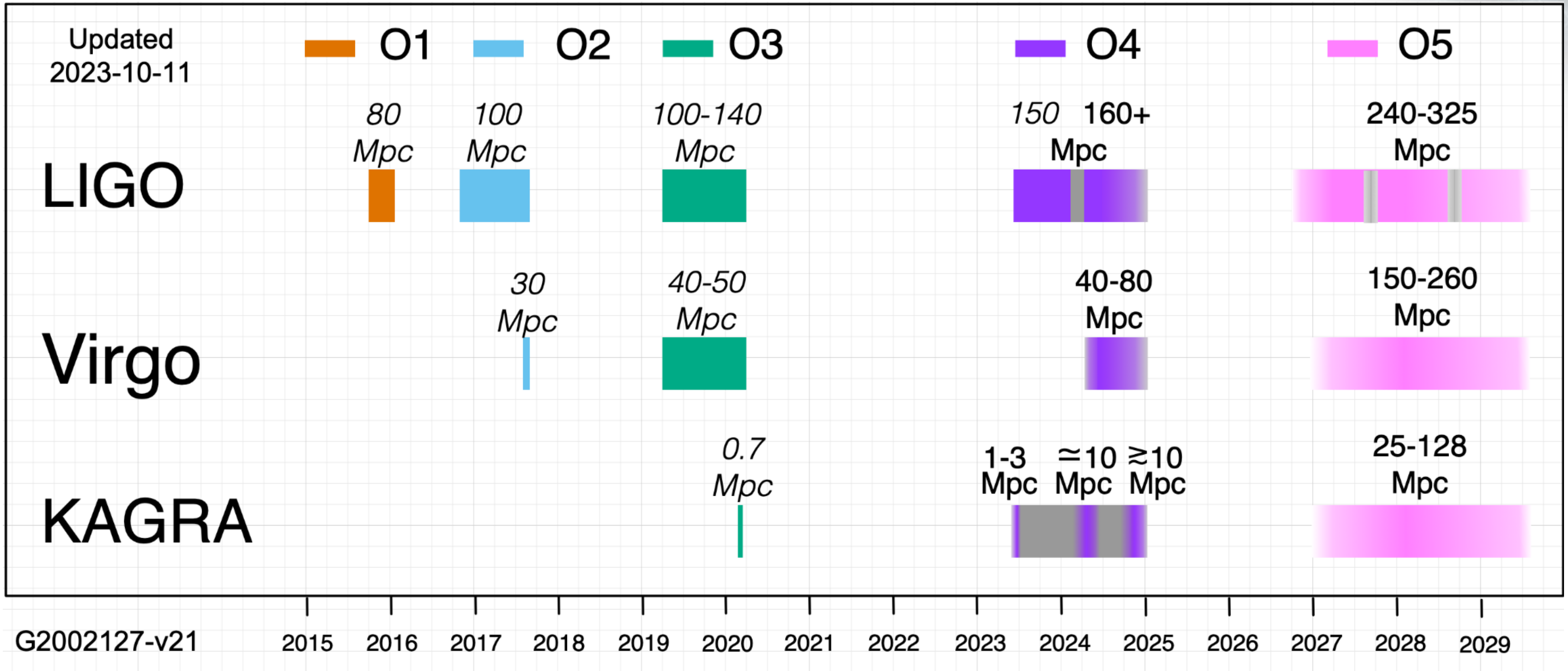

The rate density of compact binary coalescences

Compact binary star systems can emit detectable Gravitational Waves (GW) in the last stages of their inspiral motion.

- **BNS**: two Neutron Stars (NSs) system, *e.g.* GW170817;
- **NSBH**: binary formed by one Neutron Star and one Black Hole (BH), *e.g.* GW200105 and GW200115;
- **BBH**: two Black Holes (BHs) system, *e.g.* GW150914.

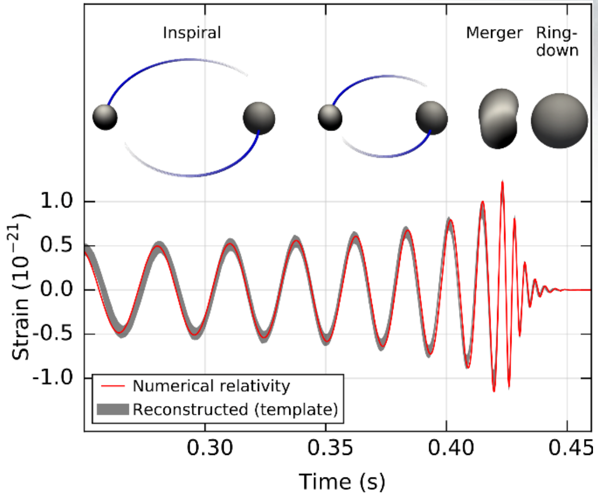

PhysRevLett.116.061102

Abadie2010

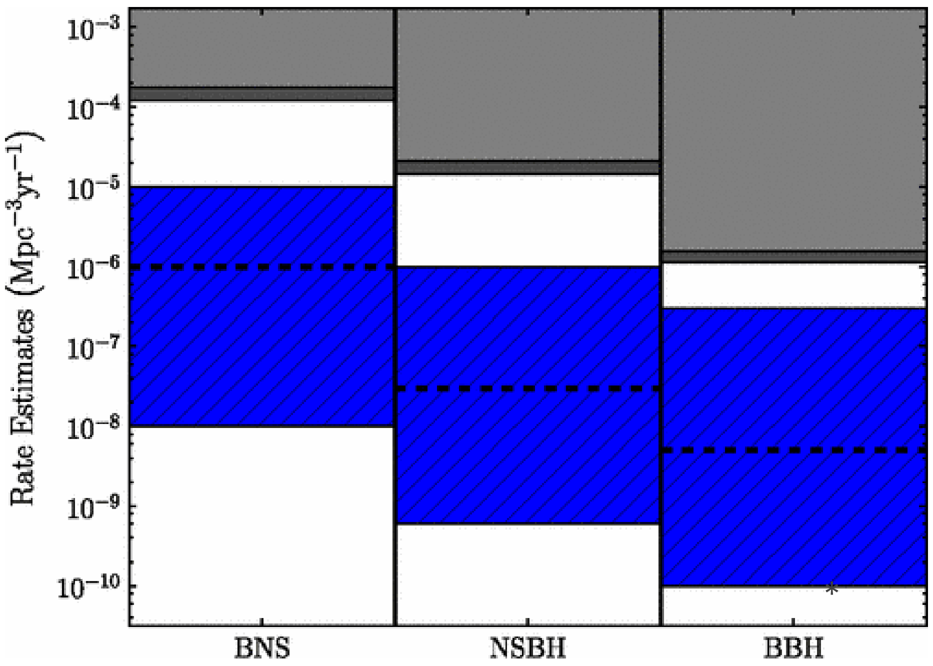

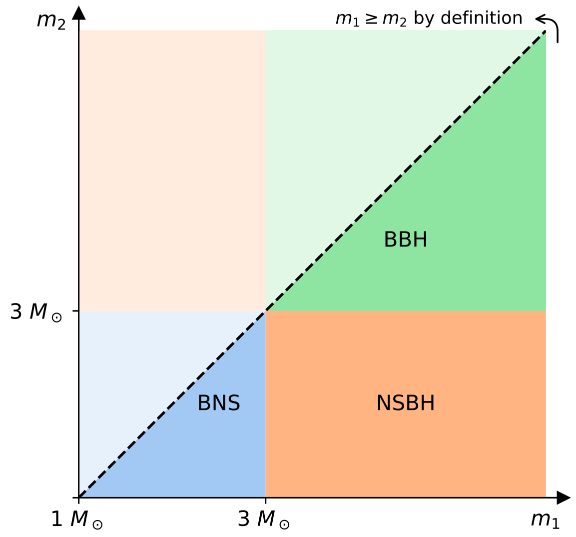

Abbott2013

*Updated inference on BBH population arXiv2010.14533

The effective BNS Volume-Time

Euclidean sensitive volume of the second-most sensitive detector in the network at a given time, multiplied by the **live time** of that network configuration.

The **network Euclidean sensitive volume** is the volume of a sphere with a radius given by the **BNS inspiral range.**

⇒ Multiplying the BNS Volume-Time by the **CBC density rate** we get an estimate of the expected number of detections. (ignoring cosmological corrections)

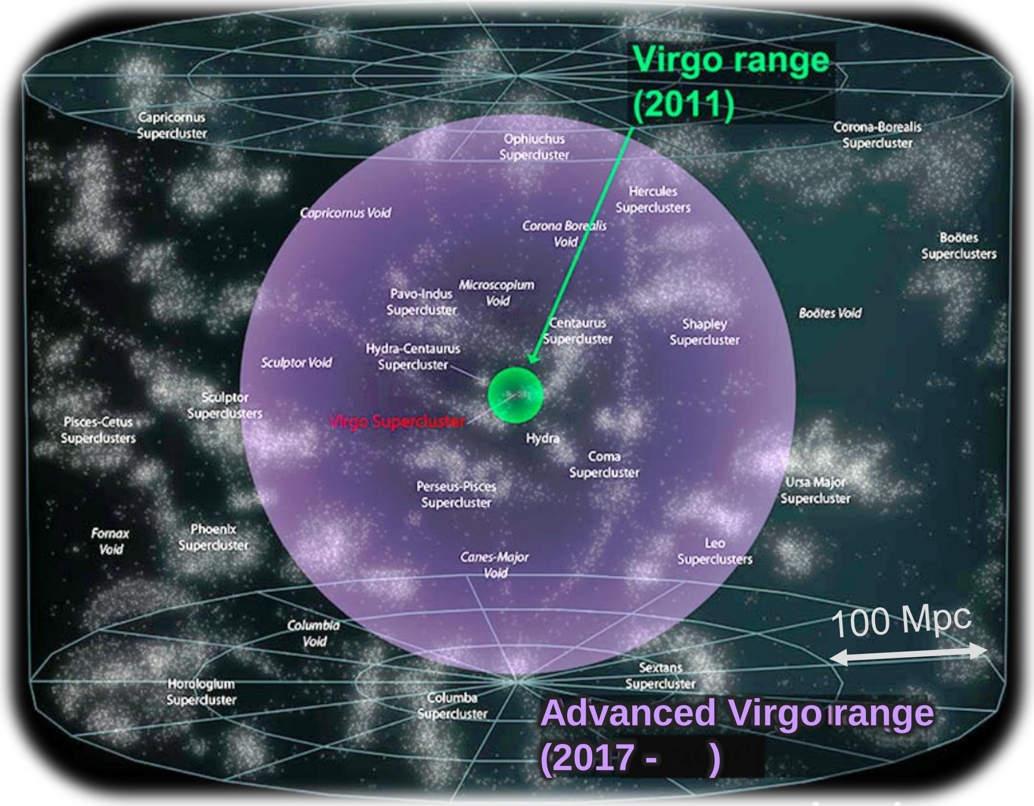

Image Credit: [Virgo Collab.]

LIGO-Virgo Network duty cycle during O3

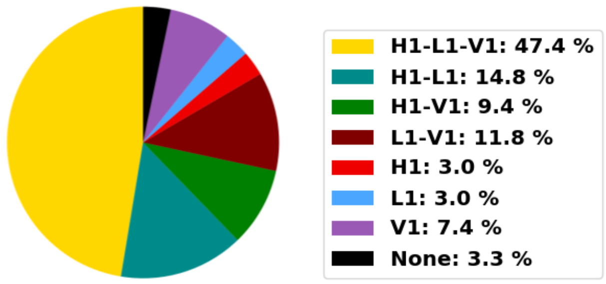

Known compact object masses vs. estimated distance

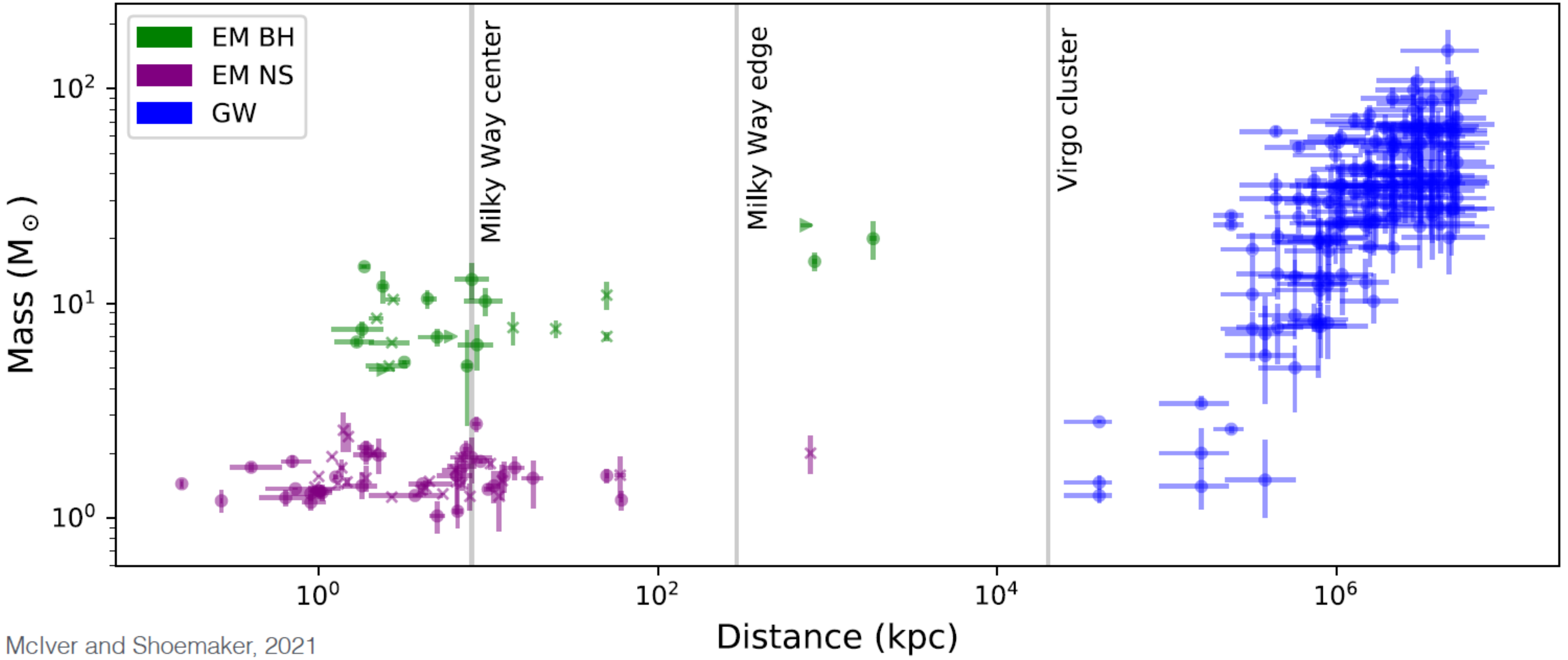

McIver and Shoemaker, 2021

Using Deep Learning to distinguish signal and noise

Multilabel classifier to label excess energy in the spectrogram images and distinguish noise artefacts from GW transients.

- Refer also to Gravity Spy and GWitchHunters projects on Zooniverse

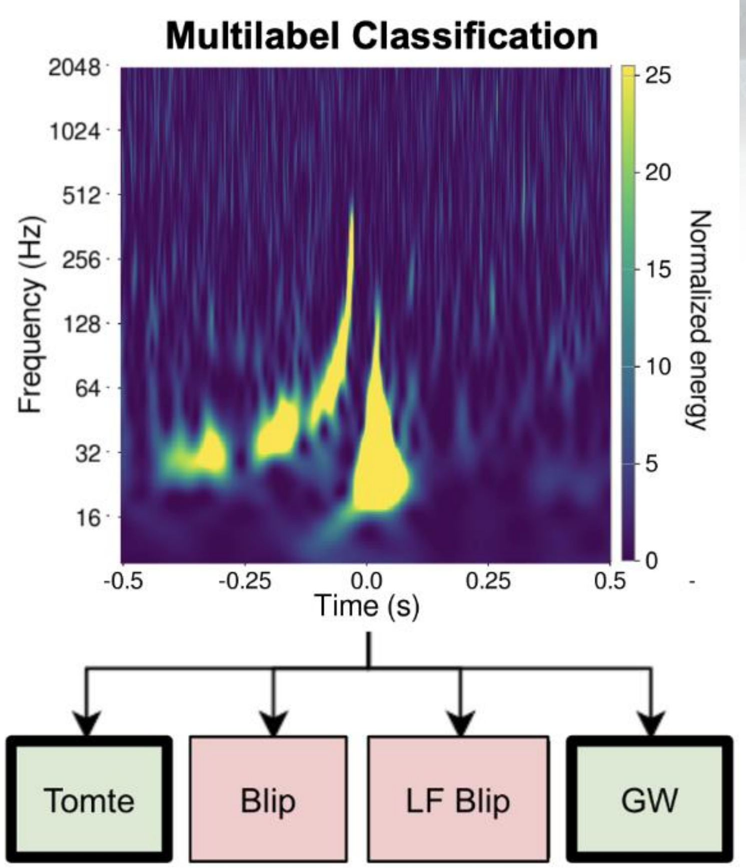

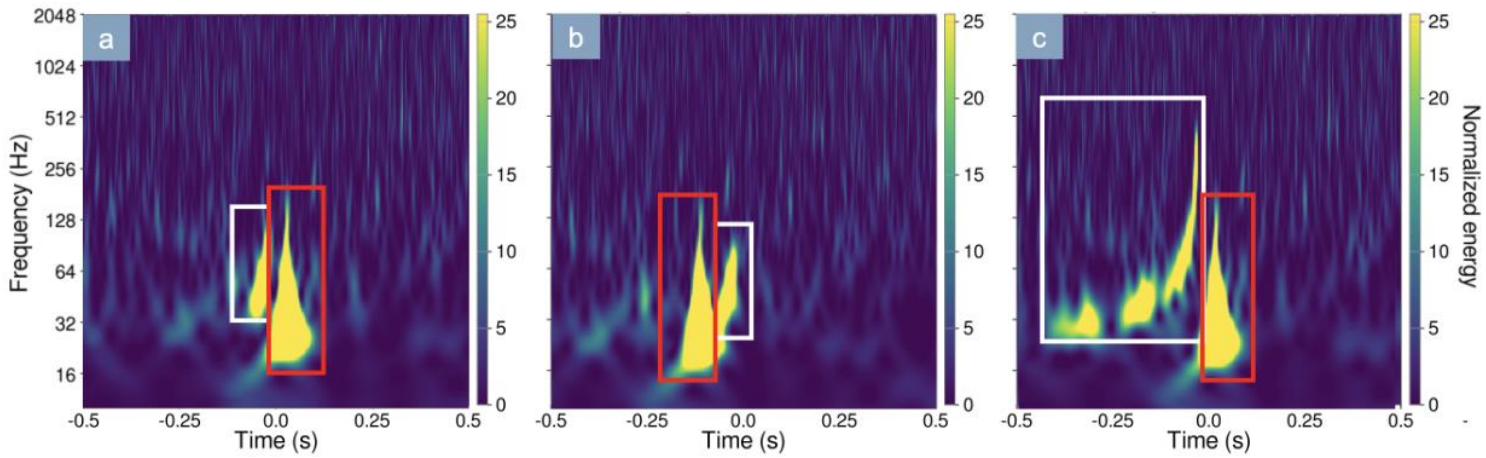

https://arxiv.org/abs/2304.09977